INFORMATION TO USERS

This manuscript has been reproduced from the microfilm master. UMI films the text directly from the original or copy submitted. Thus, some thesis and dissertation copies are in typewriter face, while others may be from any type of computer printer.

The quality of this reproduction is dependent upon the quality of the copy submitted. Broken or indistinct print, colored or poor quality illustrations and photographs, print bleedthrough, substandard margins, and improper alignment can adversely affect reproduction.

In the unlikely event that the author did not send UMI a complete manuscript and there are missing pages, these will be noted. Also, if unauthorized copyright material had to be removed, a note will indicate the deletion.

Oversize materials (e.g., maps, drawings, charts) are reproduced by sectioning the original, beginning at the upper left-hand corner and continuing from left to right in equal sections with small overlaps.

Photographs included in the original manuscript have been reproduced xerographically in this copy. Higher quality 6" x 9" black and white photographic prints are available for any photographs or illustrations appearing in this copy for an additional charge. Contact UMI directly to order.

ProQuest Information and Learning
300 North Zeeb Road, Ann Arbor, MI 48106-1346 USA
800-521-0600

Université d'Ottawa · University of Ottawa

The Light Chain of MAP1A Binds to and Stabilizes Microtubules

By

Nicoleta H. Ungureanu

A thesis submitted to the Faculty of Graduate and Postdoctoral Studies, University of Ottawa, in partial fulfillment of the requirements for the degree of Master of Science, Ottawa-Carleton Institute of Biology

September, 2001

I hereby declare that I am the sole author of this thesis.

I authorize the University of Ottawa to lend this thesis to other institutions or individuals for the purpose of scholarly research.

I further authorize the University of Ottawa to reproduce this thesis by photocopying or by other means, in total or part, at the request of other institutions or individual for the purpose of scholarly research.

Nicoleta H. Ungureanu

For Lara

ACKNOWLEDGEMENTS

I would like to thank my supervisor, Dr. David L. Brown, who provided me with a challenging research project. I am grateful for everything I learned under his supervision, and I appreciate his patience.

I would like to thank the members of my advisory committee, Dr. Jim Cheetham, Dr. Doug Johnson, and Dr. Vance Trudeau for their input into this thesis. I am grateful for Miguel Providentti's and Dr. Johnny Basso's valuable advice on molecular techniques.

I would like to thank the members of Dr. Brown's lab: Tania Villeneuve, Eric Campos, Sandra Hurley, Lise Beauchamp, Shahin Negari, and Elliott Faller for taking me as I am and for creating a "crazy" and warm atmosphere. I would like to extend special thanks to Allison Hunter for being such a great friend; I appreciate her guidance and support. I would also like to thank Andrew Ochalski for the hours of computer and microscopy trouble shooting.

I would also like to thank Nisrine Haddad, Corrado Selva, and Mehrdad Hajibabei for always being there for me, and to Ariane Beauvais and Parisa Aghsani for their kindness.

I would like to thank all my weird, but dear friends, both in Romania and here in Canada, my small but very important family, and my stubborn but supportive husband, Fritz, who all together contributed, in one way or another, to who I am.

TABLE OF CONTENTS

ABBREVIATIONS

AA	amino acid
α-MEM	α-modified Eagle's minimal essential media
BSA	bovine serum albumin
CCD	charge-cooled device
cDNA	complementary deoxyribonucleic acid
cs	coverslip
CY2	carboxymethylindocarbocyanine
CY3	indocarbocyanine
ddH_2O	double distilled, deionized water
DMSO	dimethyl sulfoxide
DNA	deoxyribonucleic acid
DTT	dithiothreitol
EC	embryonal carcinoma
ECL	enhanced chemiluminescence
EDTA	ethylenediaminetetraacetic acid disodium salt
EGTA	ethyene glycol bis (β-aminoethylether)
FCS	fetal calf serum
GTP	guanidine triphosphate

HMW	high molecular weight
HRP	horse radish peroxidase
IMW	intermediate molecular weight
kb	kilobase
kDA	kilodalton
LB	Luria Bertani
LC	light chain
LMW	low molecular weight
mAb	monoclonal antibody
MAP	microtubule-associated protein
mRNA	messenger ribonucleic acid
MES	N-morpholinoethanesulfonic acid
MT	microtubule
MTOC	microtubule organizing center
MW	molecular weight
NC	nitrocellulose
ON	overnight
pAb	polyclonal antibody
PBS	phosphate buffered saline
PC	phosphocellulose
PEFA	p-aminoethylbenzenesulfonyl fluoride

PEM	PIPES/EGTA/$MgCl_2$ buffer
PIPES	piperazine-N.N'-bis-2-ethanesulfonic acid
RT	room temperature
SDS-PAGE	sodium dodecyl sulfate polyacrylamide gel electrophoresis
TIFF	tagged image file format

LIST OF FIGURES

ABSTRACT

Microtubule-associated protein 1A (MAP1A) is expressed in the nervous system during development and its expression parallels an increase in microtubule (MT) stability. Previous studies (Vaillant et al., 1998) revealed that the entire MAP1A protein complex represented by heavy chain and light chain (LC2) and the MAP1A heavy chain alone bind to MTs and have moderate effects on MT stability. To determine if LC2 alone can bind to MTs *in vivo*, we expressed EGFP-tagged LC2 by transient transfection in HeLa cells. Fluorescence microscopy showed that EGFP-LC2 binds to MTs and alters their distribution. EGFP-LC2 had some effect on intermediate filament distribution, but no effect on actin. EGFP-LC2 also induced formation of stable MTs, as shown by their resistance to the effects of nocodazole and taxol. Co-transfection studies showed that LC2 bound to the N-terminus (AAs 1-281) of MAP1A heavy chain, and that the heavy chain might regulate LC2 activities, by greatly reducing LC2 effects on MTs.

RESUME

La protéine associée aux microtubules 1A (MAP1A) est exprimée de façon développementale dans le système nerveux. Son expression parallèle une augmentation dans la stabilité des microtubules (MT). Des études précédentes (Vaillant et al., 1998) ont démontrées que la structure entière de MAP1A, comprenant la chaine lourde et la chaine légère (LC2), ainsi que la chaine lourde seule se lient aux MTs mais ont peu d'effet sur la stabilité des MTs. Pour déterminer si LC2 par soi-même se lie aux MTs *in vivo*, LC2 conjugé à EGFP a été exprimé par transfection transiente dans des cellules HeLa. La microscopie fluorescente a démontrée que LC2-EGFP se lie aux MTs et modifie leur distribution. LC2-EGFP modifie la distribution des filaments intermédiaires, mais a aucun effet sur l'actine. LC2-EGFP a aussi causé la formation de MTs stables, résistantes à les drogues nocodazole et taxol. Des études de co-transfection ont démontrées que LC2 se lie aux terminus N (AAs 1-281) de la chaine lourde de MAP1A et que la chaine lourde régle les activités de LC2.

I. INTRODUCTION

A. Microtubules: Stability and Instability

Microtubules (MTs) are cylindrical organelles, found in all eukaryotes in almost all cell types. They interact with microfilaments and intermediate filaments to form a three-dimensional network, the cytoskeleton. The MT building block subunit is the 100 kDa protein, tubulin. The tubulin molecule is a heterodimer of two 50 kDa polypeptide chains, designated α and β (Ludueña, 1998, for review). The tubulin dimers associate in a head-to-tail fashion to form linear protofilaments. Typically, 13 protofilaments, whose axes are parallel to that of the MT, associate laterally to form a tube of 24 nm in diameter (Laferrière et al., 1997, for review) (**Fig.1**).

Not only do MTs have a ubiquitous distribution, but they also perform in a wide variety of functions that are essential for cellular life. On the one hand, MTs serve primarily cytoskeletal functions, being involved in generation and maintenance of cell shape. On the other hand, they are involved in a variety of other cellular processes, including chromosome segregation during mitosis and meiosis, ciliary and flagellar motility, and distribution and transport of vesicles and organelles (Chapin and Bulinski, 1992; Ludueña, 1998, for reviews).

To participate in such a variety of cellular functions, MTs exhibit a full range of stability states (Margolis and Job, 1994, for review). These highly variant stability states represent the consequences of the inherent behavior

Figure 1: Schematic representation showing the arrangement of tubulin dimers in the assembled MT (Reproduced from Vaillant, 1997).

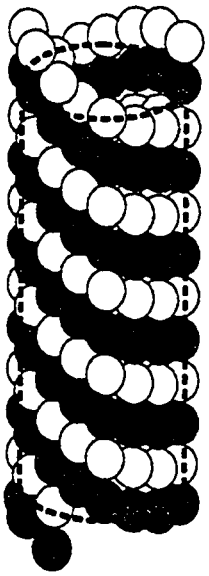

SIDE VIEW OF A MICROTUBULE

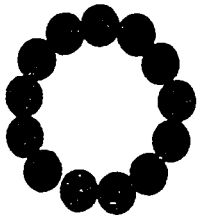

CROSS SECTION OF A MICROTUBULE

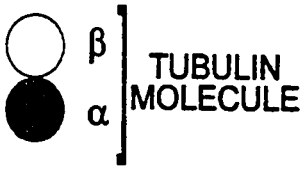

of MTs, best described by the dynamic instability model, proposed by Mitchison and Kirchner (1984). According to this model MTs are labile polymers that exist, both *in vitro* and in living cells, in one of two phases: either elongating, by the addition, or shortening, by the loss of tubulin heterodimers from the MT ends. As the transition from elongation to rapid shortening (catastrophe) and the transition from rapid shortening to elongation (rescue) alternate and occur in an abrupt and random manner, the entire MT population behaves heterogeneously (Cassimeris, 1993).

MT heterogeneity in different cells and even within a single cell is thought to be temporally and spatially modulated, either singly or in combination, by a multiplicity of factors that alter the frequencies of catastrophe and rescue. The expression of multiple α and β tubulins encoded by distinct genes, posttranslational modification of α and β tubulins (phosphorylation, acetylation, tryrosination/detyrosination, polyglutamylation, polyglycylation), and the expression or modification of various microtubule-associated proteins (MAPs) appear to modulate MT dynamics (Wordeman and Mitchison, 1994; Laferrière et al., 1997; Ludueña, 1998, for reviews).

Based mainly on *in vitro* studies, accumulated evidence indicates that structural MAPs represent the major tissue- and development- specific regulators of MT stability *in vivo* (Chapin and Bulinski, 1992; Maccini and Cambiazo, 1995, for reviews).

B. Microtubule –Associated Proteins (MAPs)

MAPs form a large and heterogenous group of proteins found to co-purify in a constant stoichiometry with tubulin during repeated cycles of temperature-dependent MT assembly/disassembly and during taxol-stimulated MT assembly *in vitro* (Schoenfeld and Obar, 1994, for review). They can be diverse, but certain MAPs share common features and probably work by similar mechanisms. Based on whether or not their MT binding is sensitive to nucleotides (ATP, GTP), all MAPs from higher organisms can be categorized into two groups: motor MAPs, whose MT binding is nucleotide sensitive, and structural MAPs , whose MT binding is not influenced by nucleotides (Chapin and Bulinski, 1992; Maccini and Cambiazo, 1995, for reviews).

Consequently, the two groups of MAPs are involved in different cellular processes. Interacting with MTs, the group of motor MAPs (that include the dynein and kinesin families of proteins) is involved in motile cellular functions (mitosis and meiosis, organelle movement and flagellar-based motility), by converting the energy of ATP into mechanical energy of movement (Vale, 1990, for review). Binding to MTs, the group of structural MAPs (that include the major MAPs: MAP1, MAP2, MAP3, MAP4 and tau) stimulate MT assembly both *in vitro* and *in vivo*, and affect MT stability and MT interaction

Table I: MAP isoforms of the nervous system: localization, and expression (adapted from Riederer, 1990, Doll et al., 1993, and Schoenfeld and Obar, 1994)

Species	Isoforms*	MW (kDa)	Nervous System Localization	Expression During Neuronal Differentiation
MAP1A		350	dendrites, soma & axons	late
MAP1B		330	dendrites, soma & axons	early
MAP2	MAP2a	280	dendrites & soma	late
	MAP2b	260	dendrites & soma	early & late
	MAP2c	70	dendrites, soma & axons	early
	MAP2d	74	glial cells	late
tau	multiple (6)	45-65	preferentially in axons	early (juvenile forms) late (adult forms)

*They are generated by alternative mRNA splicing

Figure 2: Schematic representation showing the two functional regions of structural MAPs (Reproduced from Vaillant, 1997).

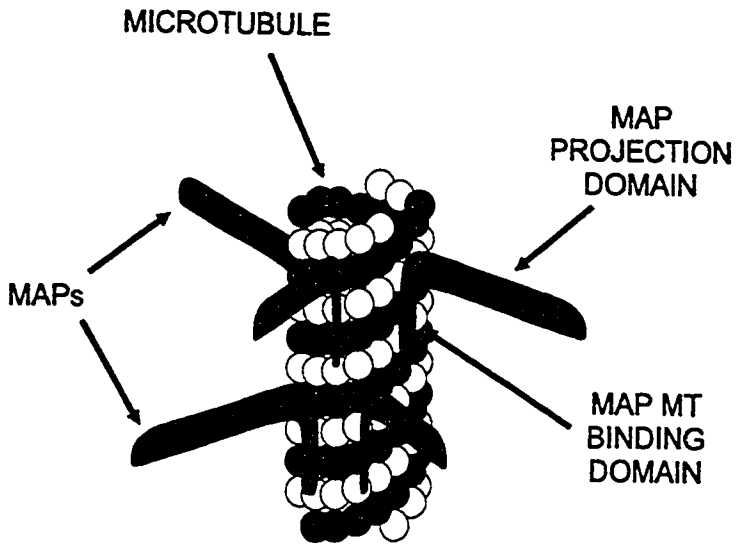
MICROTUBULE
MAP
PROJECTION
DOMAIN
MAPs
MAP MT
BINDING
DOMAIN

with other cellular components (Chapin and Bulinski, 1992, Maccini and Cambiazo, 1995, for reviews).

C. Structural MAPs

The majority of the structural MAPs are particularly prominent in the nervous system, from where they were initially isolated (Maccini and Cambiazo, 1995, for review) **(Table I)**. Ultrastructural studies of MAPs incorporated into tubulin polymers demonstrated that structural MAPs are fibrous molecules of different lengths (50nm to 185nm) that form lateral projections from the MT surface (**Fig.2**).

Structural MAPs are asymmetric molecules with two functional regions: 1) an acidic domain, the projection domain, that binds to other components of the cytostructure, and 2) a highly basic domain, the MT binding domain, that binds to tubulin (Maccini and Cambiazo, 1995, for review).

Structural MAPs have been classified according to many criteria. Traditionally, they were categorized according to their apparent MW into three molecular mass classes: high (HMW)(±300kDa), intermediate (IMW)(±200kDa), and low (LMW) (±100kDa) (Wiche et al., 1991; Schoenfeld and Obar, 1994, for reviews) (**Table I**). At present, as a number of MAPs have been cloned and sequenced, the major vertebrate structural MAPs can be more meaningfully classified according to their sequence homology

Table II: The two principal structural MAP families.

Family	MT -Binding Domain	Reference
Tau-MAP2-MAP4	- located near C-terminus of each molecule; - consists of two regions: 1) three to four 18-amino acid repeats; 2) the regions flanking these repeats	Gustake et al., 1994; Goedert et al., 1996.
MAP1	- located near N-terminus of each molecule; - consists of two regions: 1) eleven /twenty-one repeats of (K/R) (K/R) (E/D) motif ; 2) the regions flanking these repeats	Noble et al. ,1989; Vaillant et al.,1998.

and function into two families: the τ-MAP2-MAP4 family and the MAP1 family (Chapin and Bulinski, 1992; Müller et al. 1994, for reviews) (**Table II**).

C.1. *The τ-MAP2-MAP4 Family*

τ and MAP2 proteins, except for MAP2d isoform (Doll et al., 1993), are localized in the nervous system and are believed to be neuron specific MAPs (Gustake et al., 1994). Immunocytochemical studies demonstrated that MAP2, the most abundant brain-specific MAP, is generally localized in dendrites and somata, whereas τ protein has been found in axons (Shoenfeld and Obar, 1994, for review). By contrast, MAP4, originally isolated and characterized from HeLa cells, is the major MAP of many types of dividing cells (Gustake et al., 1994).

The thermostable proteins τ, MAP2 and MAP4 derive from different genes and additional τ, MAP2 and MAP4 isoforms are generated by alternative mRNA splicing, the type and their number varying from species to species. The pattern of τ, MAP2 and MAP4 proteins is developmentally regulated, the size and complexity of isoforms increasing with age (Goedert et al., 1996; Nguyen et al., 1997).

Molecular cloning and sequencing of τ, MAP2 and MAP4 proteins have led to the characterization of their corresponding MT binding domains. Based on these studies, the MT binding domain has been localized at a similar

position, near the carboxyl-terminus of each molecule. High sequence similarity in the MT binding domain of these three proteins has also been demonstrated (Gustake et al., 1994; Goedert et al., 1996).

The conserved region consists of a repeated 18-amino acid motif, separated by less highly conserved spacer segments. The regions flanking these repeats also present considerable sequence similarity in the case of the neuron-specific τ and MAP2, whereas MAP4 is unique in these regions. Additional studies, using *in vitro* translation products, fusion proteins and synthetic peptides, demonstrated that the MT binding domain of the tau-MAP2-MAP4 family consists of two regions: the repeat-bearing region and the regions flanking these repeats (Chapin and Bulinski, 1992, for review).

Based on extensive studies, the τ-MAP2-MAP4 family represents the best known MAP proteins. At present, there are insights not only into the structure of the τ-MAP2-MAP4 family but also into their function. Transfection of tau and MAP2 cDNA into non-neuronal culture cells demonstrated that these MAPs not only bound to non-neuronal MTs but also increased the stability and, consequently, changed the organization of MTs, by inducing the formation of MT bundles, resembling the bundled MTs found in neuronal processes. Moreover, Sf9 cells expressing τ or MAP2 extended neuron-like processes (Matus, 1994; Goedert et al., 1996, for reviews). On the contrary, cultured cells were inhibited in their extension of processes if the levels of τ

or MAP2 were decreased by anti-sense strategies. These data suggest that τ and MAP2 may play a role in neuronal morphogenesis (Goedert et al., 1996; Nguyen et al., 1997).

Despite the structural similarities of MAP4 to tau and MAP2, previous investigations of MAP4 functions *in vivo* provided contradictory information on its ability to stabilize MTs (Barlow et al., 1994; Olson et al., 1995). However, based on recent studies of permanently transfected cell lines expressing full-length MAP4 or only its MT binding domain, it has been demonstrated that MAP4 also increased MT stability, but at low levels. In addition, the permanently transfected cells grew significantly more slowly than control cells. These data suggest that MAP4 may play a role in the regulation of non-neuronal cell growth (Nguyen et al., 1997).

C.2. *The MAP1 Family*

The use of monospecific probes demonstrated that MAP1 species are found in a wide variety of cell and tissue types, but they represent the most prominent MAPs in neuronal cells (Chapin and Bulinski 1992; Műller et al., 1994, for reviews). The MAP1 structural proteins have been found to be prominent in both axons and dendrites, as well as in somata (Schoenfeld and Obar, 1994, for review). The expression of MAP1A in neurons is developmentally regulated and is complementary to that of the closely

related MAP1B (Müller et al., 1994, for review). MAP1B appears in the initial phase of neuronal differentiation and MAP1A appears later during neuronal development (Langkopf et al., 1992). According to their time of appearance, it was suggested that MAP1B plays an important role in regulating the dynamic assembly of MTs during neurite outgrowth, whereas MAP1A plays a morphological role in stabilizing the MTs in mature axons and dendrites (Müller et al., 1994, for review).

The thermolabile proteins MAP1A and MAP1B are encoded by separate genes, and they represent protein complexes of one high molecular weight polypeptide, the heavy chain, and up to three low molecular weight subunits, the light chains (LCs): LC1 (Mr=34kDa), LC2 (Mr=30kDa) and LC3 (Mr=18kDa). The association of the LCs with MAP1A and MAP1B was first deduced when the low molecular weight polypeptides were found to co-purify with the MAP1 fraction by column chromatography (Vallee and Davis, 1983; Kuznetsov and Gelfand, 1987). Further investigation, by co-immunoprecipitation of LCs with MAP1A and MAP1B, established that all three light chains were present in the MAP1A immunoprecipitates and that only LC1 and LC3 were present in the MAP1B immunoprecipitates (Kuznetsov et al., 1986, Schoenfeld et al., 1989).

Two groups have reported on subunit stochiometry of the LCs to heavy chains in MAP1 proteins (Schoenfeld et al., 1989; Pedrotti and Islam, 1994;

Pedrotti et al., 1996a). The exact stoichiometry is not known since there were differences in the techniques employed in these two studies. However, both groups suggested that the heavy chains can bind more than one copy of each LC (Hammarback, 1997, for review).

Proteolytic degradation (with α-chymotrypsin) of MAPs attached to MTs revealed a 20kDa MT bound fragment (Kuznetsov et al., 1986), derived from MAP1B heavy chain (as evidenced by its reactivity with anti-MAP1B monoclonal antibody), and a 60kDa MT bound fragment, that appeared to be derived from MAP1A heavy chain (Schoenfeld et al., 1989). Along with these fragments, LCs also remained bound to MTs, suggesting that they are associated at the MT binding end of the heavy chains (Schoenfeld et al., 1989; Hammarback et al., 1991).

Analysis of the cDNA sequence encoding the conserved carboxyl-terminal region of MAP1A and 1B and comparison of the LC amino acid sequence obtained from Edman degradation revealed that LC1 is encoded in the 3'end of the open reading frame of MAP1B (Hammarback et al., 1991); whereas, LC2 is encoded in the 3'end of the open reading frame of MAP1A (Langkopf et al., 1992). According to the polyprotein hypothesis, the single open reading frame of MAP1mRNA is translated into a single polypeptide corresponding to the full length of the open reading frame, which is then cleaved during or after translation to yield one copy of a heavy chain and one

Figure 3: Schematic representation of the proteolytic processing of the MAP1A/LC2 and MAP1B/LC1 polyprotein precursor (Reproduced from Műller et al., 1994).

MAP1 - LIGHT CHAIN PROCESSING

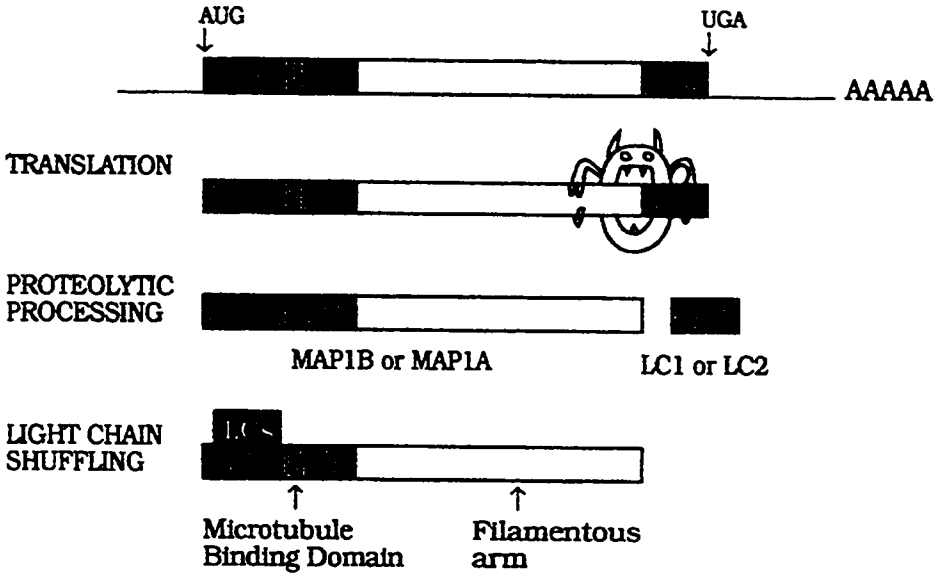

copy of the light chain (Hammarback, 1997, for review) (**Fig.3**).

Sequencing of cDNA encoding rat LC3 demonstrated that it is not found in the MAP1A/LC2 or MAP1B/LC1 polypeptide cDNA, but is encoded by a separate gene. Despite this, LC3 is always co-expressed throughout brain development with either MAP1A or MAP1B, as shown by immunocyto-chemical studies (Mann and Hammarback, 1994; 1996).

Analysis of cDNA and comparison of the deduced amino acid sequences of MAP1A and MAP1B also revealed that these two proteins are structurally related with segments exhibiting sequence identity (Langkopf et al., 1992; Fink et al., 1996). Based on transient transfection of cultured cells with cDNAs corresponding to truncated forms of MAP1A/1B and on *in vitro* microtubule binding analysis, it has been established that for both MAP1A and MAP1B the MT binding domain is located near the amino-terminus of the heavy chain (Noble et al., 1989; Vaillant et al., 1998).

The amino-terminus region of the MAP1B heavy chain contains 21 copies of a charged (K/R)(K/R)(E/D) motif (**Fig.4**) that have been shown to bind to MTs *in vitro* (Noble et al., 1989). Assays for the binding of MAP1B to MTs *in vivo* by deletion showed that the charged motif was not necessary for MT binding, but when the region flanking both sides of the charged motif was also removed, MT binding was lost (Noble et al., 1989). These studies demonstrated that the MT binding domain of MAP1B heavy chain contains

Figure 4: Schematic representation of MAP1A, MAP1B and their associated LCs (Reproduced from Vaillant, 1997).

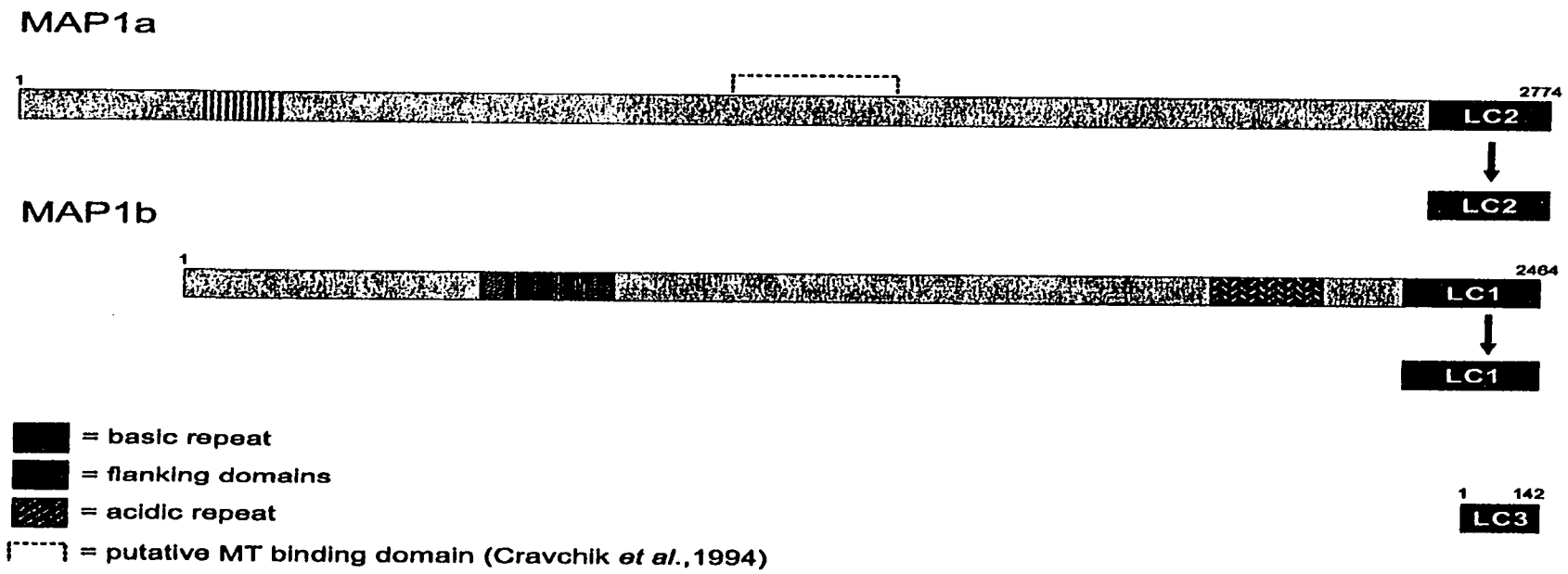
MAP1a
1
2774
LC2
LC2
MAP1b
1
2464
LC1
LC1
= basic repeat
= flanking domains
= acidic repeat
= putative MT binding domain (Cravchik et al.,1994)
1
142
LC3

two regions able to bind MTs, the (K/R)(K/R)(E/D) motif and the regions flanking these repeats (Noble et al., 1989).

The amino-terminus region of the MAP1A heavy chain also contains 11 copies of the basic (K/R)(K/R)(E/D) motif and two regions flanking the basic repeats, very similar to those in MAP1B (Langkopf et al., 1992) (**Fig.4**). Despite sequence homology at the amino-terminus of MAP1B and MAP1A, Cravchik at al. (1994) failed to detect binding to MTs of a fragment (AA 1-~1300) of MAP1A, containing the basic motif and the flanking regions. Instead, they showed binding to MTs of an acidic region near the middle of the protein (AA 1307-1606) (**Fig.4**). In contrast, in a more recent study (Vaillant et al., 1998), assays for the binding of the MAP1A to MTs both *in vitro* and *in vivo* showed that all the MAP1A fragments containing the basic repeats and the flanking regions bind to MTs (**Fig. 5**). In addition, deletion of the basic repeats did not result in loss of MT binding, demonstrating that the regions flanking the basic repeats can bind independently to MTs (Vaillant et al., 1998). These studies did not test if the basic repeats of MAP1A alone can bind MTs; however, they demonstrated that MAP1A fragments containing both the basic repeat and the flanking regions can bind to MTs both in *vitro* and *in vivo*. Based on these results, it was suggested that the MT binding domain of MAP1A heavy chain also contains two parts able to

Figure 5: Schematic showing the PGK-6myc MAP1A full length (designated PGK-6myc1a) and the PGK-6myc MAP1A heavy chain fragment expression constructs obtained by Vaillant, 1997. The PGK-6myc MAP1A heavy chain fragment vectors express: AA 1-281(PGK-6mycN1a-1), AA 1-630 (PGK-6mycN1a-2), AA 1-1310 (PGK-6mycN1a-3), AA 1-2016(PGK-6mycN1a-4), and AA 1-335 and 541-631(PGK-6mycN1a-2ΔBR) of MAP1A (Reproduced from Vaillant, 1997).

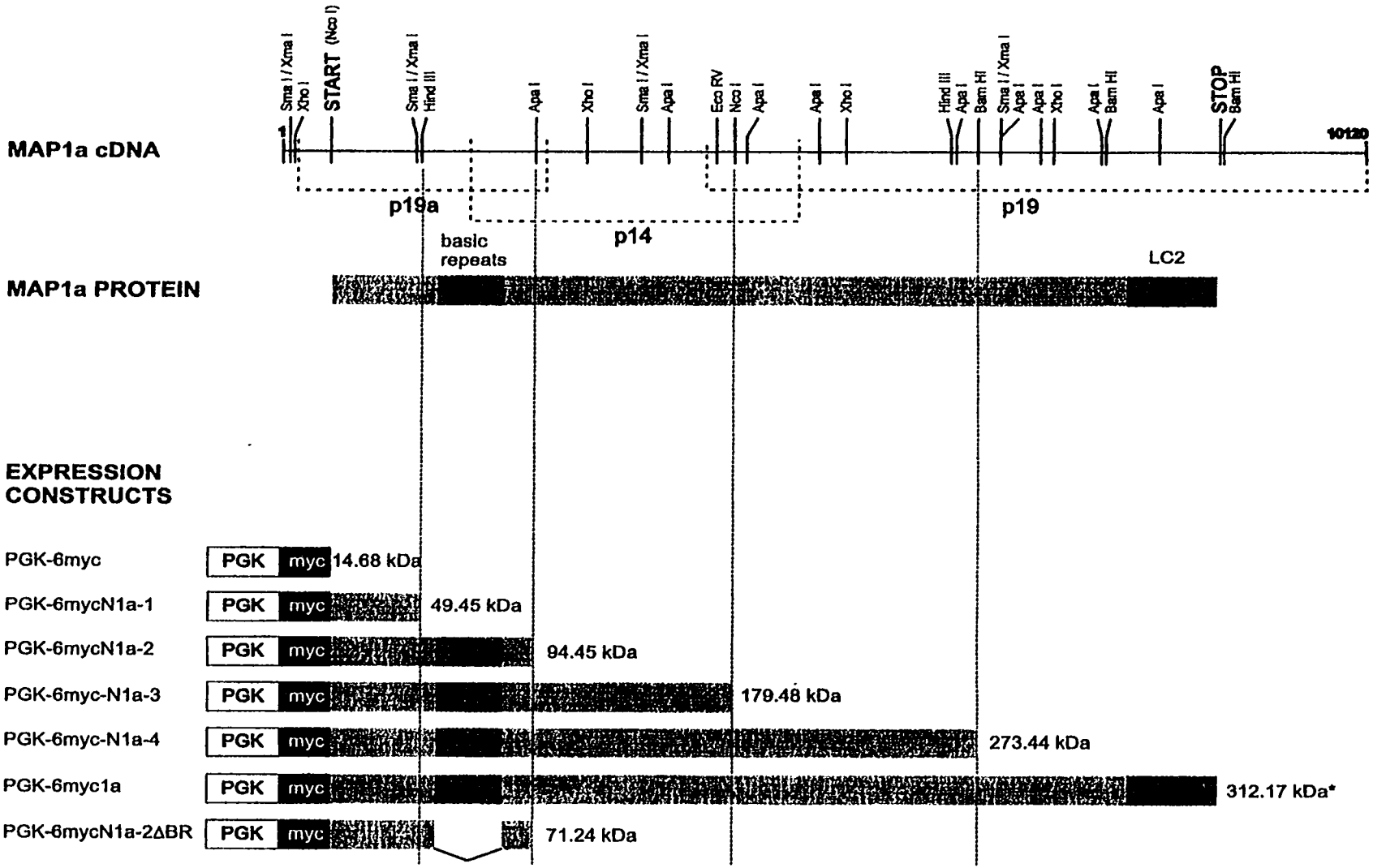
MAP1a cDNA
Sma I / Xma I
Xho I
START (Nco I)
Sma I / Xma I
Hind III
Apa I
Xho I
Sma I / Xma I
Apa I
Eco RV
Nco I
Apa I
Apa I
Xho I
Hind III
Apa I
Bam HI
Sma I / Xma I
Apa I
Apa I
Xho I
Apa I
Bam HI
Apa I
STOP
Bam HI
1
10120
p19a
p14
p19
basic repeats
LC2
MAP1a PROTEIN
EXPRESSION CONSTRUCTS
PGK-6myc
PGK
myc
14.68 kDa
PGK-6mycN1a-1
49.45 kDa
PGK-6mycN1a-2
94.45 kDa
PGK-6myc-N1a-3
179.48 kDa
PGK-6myc-N1a-4
273.44 kDa
PGK-6myc1a
312.17 kDa*
PGK-6mycN1a-2ΔBR
71.24 kDa

bind directly and independently to MTs, the basic repeated (K/R)(K/R)(E/D) motif and the regions flanking these repeats (Vaillant et al., 1998).

If there is concrete and clear evidence (see above) that the heavy chain of MAP1A/B is able to bind by itself to MTs, there are controversial experimental observations regarding the ability of the LCs to bind alone to MTs. On the one hand, preliminary studies from our laboratory (Vaillant, 1997), consisting of immunofluorescence microscopy investigation of P19EC and HeLa cells transfected with cDNA constructs for LC1, LC2 and LC3, revealed that the LCs do not co-localize with the MTs. On the other hand, analysis of the capacity of radiolabeled recombinant MAP1B fragments synthesized in bacteria to cosediment with MTs *in vitro* demonstrated that the protein sequence spanning LC1 binds directly to MTs (Zauner et al., 1992). Moreover, recent investigations (Tőgel et al., 1998) by immuno-fluorescence microscopy of cells transiently transfected with cDNA corresponding to LC1, in the absence or presence of the MAP1B heavy chain, revealed that LC1 co-localizes with MTs *in vivo*. In addition, in the same study (Tőgel et al., 1998), it has been demonstrated that a fragment corresponding to the C terminus of the LC1 was able to co-localize alone with actin stress fibers and, furthermore, that it targets to the actin fibrers the otherwise diffusely distributed N terminus of the MAP1B heavy chain.

There are some insights into the functions of MAP1A and MAP1B.

Biochemical studies revealed that both MAP1A and MAP1B were able to promote efficient MT assembly. The rates of MT assembly and disassembly in the presence of MAP1A or MAP1B were higher than those in the presence of MAP2 (Pedrotti et al., 1993; Pedrotti and Islam, 1994; Pedrotti et al., 1996a). In addition, *in vivo* studies with transfected cultured cells also showed that MAP1A/MAP1B MTs were more dynamic than MAP2 MTs (Takemura et al., 1992; Vaillant et al., 1998). These experimental results suggested that MAP1A and MAP1B were weaker MT stabilizers compared with MAP2. Beside their stabilizing activity, MAP1A/B proteins also affected MT morphology. Electron microscopic investigations of MTs assembled in the presence of MAP1A revealed that they were short and straight and differed from those assembled in the presence of MAP1B, which were long and 'bendy'. Based on these results, it was suggested that the different MT shapes might reflect alterations in MT flexibility, induced by MAP1A/B (Pedrotti et al., 1996b).

In vitro studies showed that MAP1A and MAP1B were able to interact with actin filaments as well as with MTs (Fuji et al., 1993; Pedrotti et al., 1994; Pedrotti and Islam, 1996). In addition, immunoelectron microscopic analysis revealed that Map1A/B proteins were components of fibrous cross-bridges between MTs in neurons (Shiomura and Hirokawa, 1987; Sato-Yoshitake et al., 1989). The interactions of MAP1A/B proteins with MTs and

actin filaments suggest an important role for these proteins in determining the organization and stability of the cytomatrix.

Recent experimental investigations suggest that MAP1B has a key role in neuritogenesis . In this respect, numerous studies on transgenic MAP1B mutant mice (Edelman et al., 1996, Takei et al., 1997; Gonzalez-Billault et al., 2000; Meixner et al., 2000), despite some differences in the severity of the effects, all demonstrated that MAP1B deficient mice have an impairment of brain development (Gonzalez-Billault et al., 2001). In addition, studies of inhibition of MAP1B expression both in PC12 cells, by employing antisense oligonucleotide technology (Brugg et al., 1993) and in cultured neurons obtained from MAP1B mutant mouse line (Gonzalez-Billault et al., 2001) demonstrated that MAP1B, by regulating MT dynamics and cytoskeletal organization, has a crucial role in axon formation (Brugg et al., 1993; Gonzalez-Billault et al., 2001). In contrast, the functions of the related MAP1A in neurons are unknown.

D. RATIONALE FOR EXPERIMENTS

MAP1A is one of the major structural MAPs in rat, hamster and human adult brains, being expressed in various brain regions (Garner et al, 1990; Langkopf et al., 1992, Fukuyama and Rapoport, 1995; Fink et al., 1996). In neurons, MAP1A is prominent in both axons and dendrites, as well as in

somata, thus, changes in its expression would appear to have global effects within neurons (Oblinger and Kost, 1994).

The expression of MAP1A is developmentally regulated, being present at higher levels in adulthood than in the fetal and neonatal stages in rat (Riederer and Matus, 1985; Garner et al. 1990), mouse (Matus, 1988), as well as human brain (Fink et al., 1996). As the increase in MAP1A expression parallels an increase in MT stability, it has been suggested that MAP1A, by stabilizing the MTs in mature neurons, indirectly plays a role in maintaining neuronal morphology (Műller et al., 1994). In addition, during differentiation, MAP1A expression reaches a maximum during the growth phase of both neurons from embryonic murine brain (Matus, 1988) and cultured P19 EC neurons (Vaillant and Brown, 1995; Vaillant, 1997). In adult brain, MAP1A is also expressed in regions where neuronal growth persists (McKerracher et al., 1989; Schoenfeld et al., 1989). These data suggest that MAP1A also has a growth-related function in neurons (Vaillant et al., 1998), similar to the function of MAP1B in neurite extension early in neuronal differentiation (Ulloa et al., 1997, for review)

The lack of information regarding the roles of its associated light chains represents one of the reasons that the functions of MAP1A are still poorly clarified. The purpose of the present study is to determine what role the LC2

plays in binding of MAP1A to MTs and what role it may play in modulating any effects of MAP1A on MT dynamics.

II. MATERIALS AND METHODS

A. MAP1A and MAP2c Expression Constructs

The PGK-6myc MAP1A and PGK-6myc MAP1A heavy chain fragment expression vectors were previously constructed by A. Vaillant using three overlapping cDNAs spanning the entire mRNA for MAP1A (Langkopf et al., 1992; see **Fig. 5** and detailed description in Vaillant, 1997; Vaillant et al., 1998). The coding sequences for the full length MAP1A and all the MAP1A heavy chain fragments were cloned into the pKJ1ΔF-6myc vector (a gift from Dr. M. McBurney, University of Ottawa), which is a pUC19-based vector, containing the constitutively active mouse phosphoglycerate kinase (PGK) promoter driving the expression of 6 repeats of a 9 amino acid epitope from the human c-MYC protein.

The pMAP2c-EGFP expression vector (**Fig.6**) was previously constructed by K. Currie in our laboratory using a 1.4kb Bgl II-Msc I fragment (containing the MT binding domain of MAP2c) from the pPGK-MAP2c plasmid, obtained by C. Addison (1997) also in our laboratory. This vector was constructed by ligating a 1.7kb fragment containing the MAP2c cDNA (Kindler et al., 1990) (a gift from Dr. C. C. Garner, University of Alabama, Birmingham). The 1.4kb fragment from it was ligated into Bgl II-Sma I cut pEGFP-N1 commercially available vector (Clontech Laboratories), which contains the CMV promoter driving the expression of the EGFP tag.

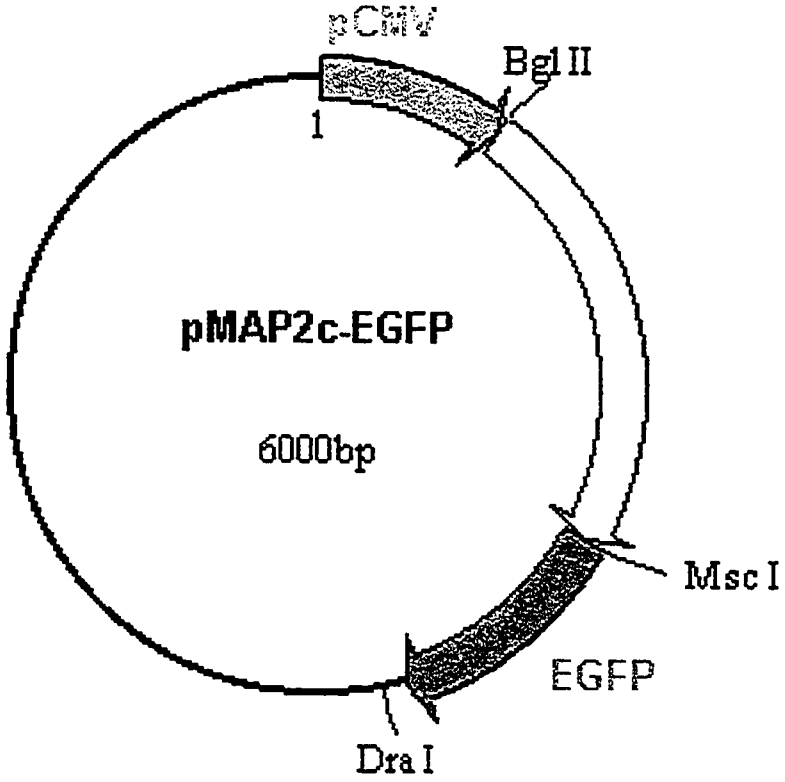

Figure 6: Map of the expression vector pMAP2c-EGFP.

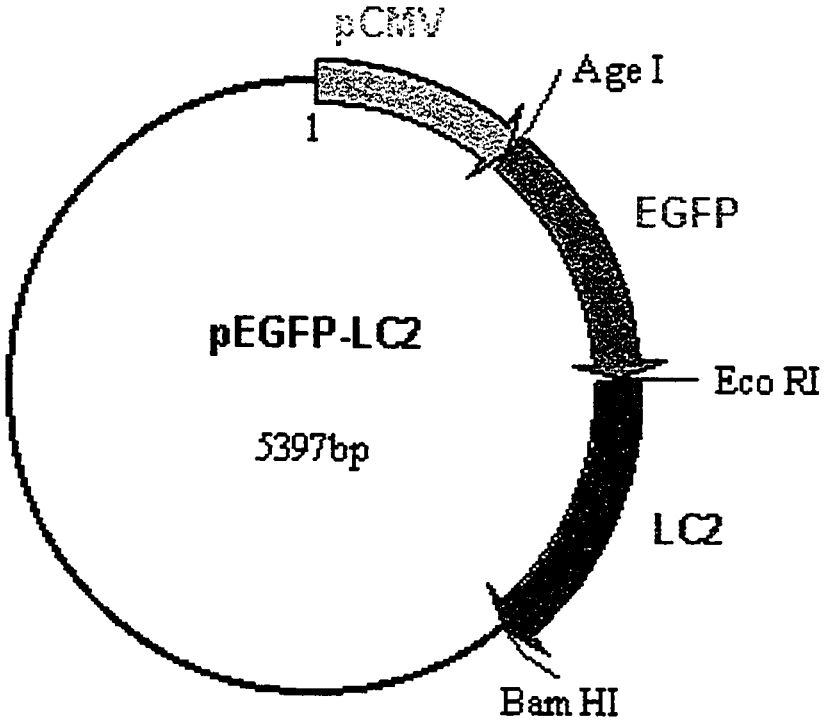

Figure 7: Map of the expression vector pEGFP-LC2.

B. Construction of the pEGFP-LC2 Expression Vector

A 666 bp Eco RI - Bam HI fragment from PGK- 6myc LC2 plasmid (obtained by A.Vaillant, 1997, using a cDNA for LC2 obtained from Dr. J. Hammarback, Bowman Gray School of Medicine, NC) was ligated into EcoRI- BamHI cut pEGFP-C_1 commercially available vector (Clontech Laboratories). The pEGFP-LC2 vector expresses the EGFP tag and amino acids 2554-2774 of rat MAP1A (**Fig. 7**), that corresponds to the region reported to be LC2 (Langkopf et al., 1992). The expression of the N-terminus fusion polypeptide is under the control of the CMV promoter.

The pEGFP-LC2 ligation product was transformed into chemically competent DH5αF´ *E.coli* (Hanahan, 1983) by heat shock according to Sambrook et al. (1989). Transformed *E. coli* were then plated onto LB agar plates supplemented with 50 µg/ml of kanamycin (Sigma) and incubated over night (ON) at 37°C. Using aseptic techniques, one colony was used to innoculated 5ml cultures of LB broth with kanamycin as above and grown at 37°C with vigorous shaking (~300rpm) to saturation (16 hours). Plasmid DNA was then harvested from each culture using the Wizard® Plus SV Minipreps kit (Promega), and screened by restriction digest (Sambrook et al., 1989). Plasimd DNA from the positive clone was then purified using the GFX™ PCR DNA and Gel Band Purification kit (Amersham) prior to sequencing.

C. Large Scale Production of Plasmid DNA for Transfection

Plasmid DNA was transformed into competent DH5αF´ *E. coli* as above. Colonies were used to inoculate 5 ml of LB cultures with either kanamycin as above, in case of the pEGFP based vectors, or 100 µg/ml ampicillin, in case of the PGK-6myc based vectors, and grown ON at 37°C, with vigorous shaking (~300 rpm). The following day, small cultures were diluted 1:500 in 500 ml LB-broth with kanamycin or with ampicillin, as above, and grown to saturation for 16 hours as above. Plasmid DNA was harvested from large cultures by centrifugation and isolated by alkaline-lysis using Qiagen Plasmid Mega kit (25) (Qiagen). The plasmid DNA was then resuspended in ddH_2O and stored at -20°C. DNA concentration and purity were determined by UV absorbance at 260 and 280nm using a Genequant® spectrophotometer (Pharmacia).

D. Tissue Culture and Transient Transfection

HeLa CCL-2 cells (ATCC) were kept semiconfluent in α-modified Eagle's minimal essential medium (α-MEM) (GIBCO BRL) supplemented with 10% FCS (Cansera) and 1% antibiotics (GIBCO). Cells were grown in a humidified incubator at 37°C and 5% CO_2 and passed every two days.

Before transient transfection, cells were seeded on 22 mm^2 glass coverslips (VWR) at a density of $5x10^4$ cells/ml, for microscopy, or on 60 mm culture dishes (Corning) at a density of $5 x10^5$ cells/ml, for protein extraction. Cells were allowed to recover for 24 h in α-MEM containing 10%FCS and 1% antibiotics. The next day, cells were transiently transfected or co-transfected using the multi-component lipid-based FuGENE 6 Transfection Reagent (Roche Molecular Biochemicals). The transfection and co-transfection mixtures were prepared, according to the manufacturer, with a FuGENE 6 Reagent (µl): DNA (µg) ratio of 3:1 in 100 µl sterile serum-free and anti-biotic-free α-MEM. The solution was gently mixed and incubated for 15 minutes at RT. Dropwise, 100µl of the complex mixture was added to each coverslip, or 200µl was added to each 60 mm dish. Cells were incubated at 37°C and 5% CO_2 a further 48 hr before processing.

E. Drug Treatments

Taxol (Sigma) was kept as a 10^{-2} M stock in DMSO at -20°C. This stock was then diluted to 5µM in α-MEM containing 10% FCS and 1% antibiotics to treat cell cultures for 7 hours. Nocodazole (Sigma) was kept as a 5mg/ml stock in DMSO at -20°C and diluted to 10µg/ml to treat the cells for 1 hour. Cytochalasin B (Sigma) was kept as a 10mg/ml stock in DMSO at

-20°C and diluted to 10μg/ml to treat the cells for 45 minutes.

F. SDS- Whole Cell Protein Extraction

This method (**Fig. 8**) was used for preparing extracts for SDS-PAGE and dot-blot analysis. Protein was extracted from cells using the method described in Drubin et al., (1985), but using higher concentration of protease inhibitors in the extraction buffer. Dishes were rinsed briefly in rinse buffer [0.13M NaCl, 2mM KCl, 8mM Na_2HPO_4, 2mM KH_2PO_4, pH7] and then 250μl of extraction buffer [25mM Na_2HPO_4, pH 7.2, 400mM NaCl, 0.5%(w/v) SDS, 40 μM benzamidine HCl (Sigma), 4 mM PEFA (Centrichem), 1mM 1,10-phenathroline (Sigma), 40 μg/ml each of apoprotinin, pepstatin A and leupeptin (all from Sigma)] was added. The viscous lysate was immediately scraped into an eppendorf tube and placed in a boiling water bath for 10 min and then spun for 10 min at 10 000 rpm and 4°C. The supernatant was removed and stored at -85°C.

G. Polymer/Soluble Protein Extraction

This method (**Fig. 9**) was used to determine if EGFP-LC2 is present in the polymerized MT fraction. Cells were rinsed briefly with 37°C pre-warmed

Figure 8: Protocol for SDS-whole cell extraction

(Reproduced from Vaillant, 1997).

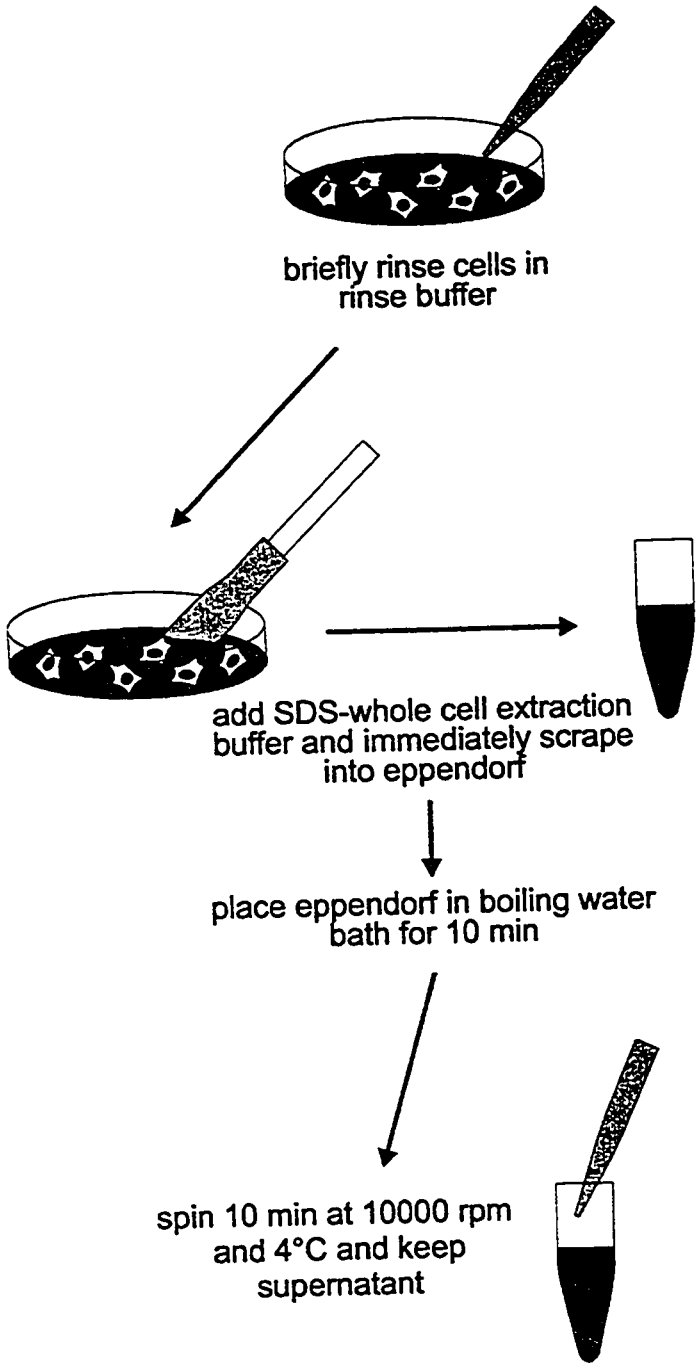
briefly rinse cells in rinse buffer
add SDS-whole cell extraction buffer and immediately scrape into eppendorf
place eppendorf in boiling water bath for 10 min
spin 10 min at 10000 rpm and 4°C and keep supernatant

PEM buffer [40 mM PIPES, pH6.8, 2.5 mM EGTA, 0.5 mM $MgCl_2$ (all from Sigma)]. Cells were then incubated for 5 min at 37°C in 250µl of microtubule stabilizing buffer [0.1M MES (Boehringer Mannheim), pH 6.75, 1mM $MgSO_4$, 2mM EDTA (Sigma), 0.1 mM EGTA, 4M glycerol (BDH), 0.5% Triton X-100 (Pierce)] (Joshi and Cleveland, 1989), including 4 mM PEFA and 40 µg/ml each of apoprotinin, pepstatin A and leupeptin (all from Sigma). The extraction buffer was then removed from the dish, pippeted into an eppendorf tube and was spun at 10,000 rpm for 2 min at room temperature. The supernatant was transferred to another tube and labelled as the soluble fraction. Then, 250µl of microtubule destabilizing buffer [0.1 M MES, 1mM $MgSO_4$, 10 mM $CaCl_2$, pH 6.9, 1mM DTT (BRL) and 5mM GTP, type II (Sigma)] (Thrower et al., 1991), also including protease inhibitors as above, was added to the dish. The buffer and the cells were scraped into the eppendorf tube containing the pellet remaining from the soluble fraction. The contents in the tube were then sonicated for 15 sec at 90-95 W using a Braun sonicator, incubated on ice for 1hr and spun at 10,000 rpm for 10 min at 4°C. The supernatant was labelled as the polymer fraction.

For all samples, protein concentrations were determined using the bicinchoninic acid protein assay (Pierce) with Bovine Serum Albumin (Pierce) diluted in ddH2O as a standard.

Figure 9: Protocol for polymer/soluble extraction

(Reproduced from Vaillant, 1997).

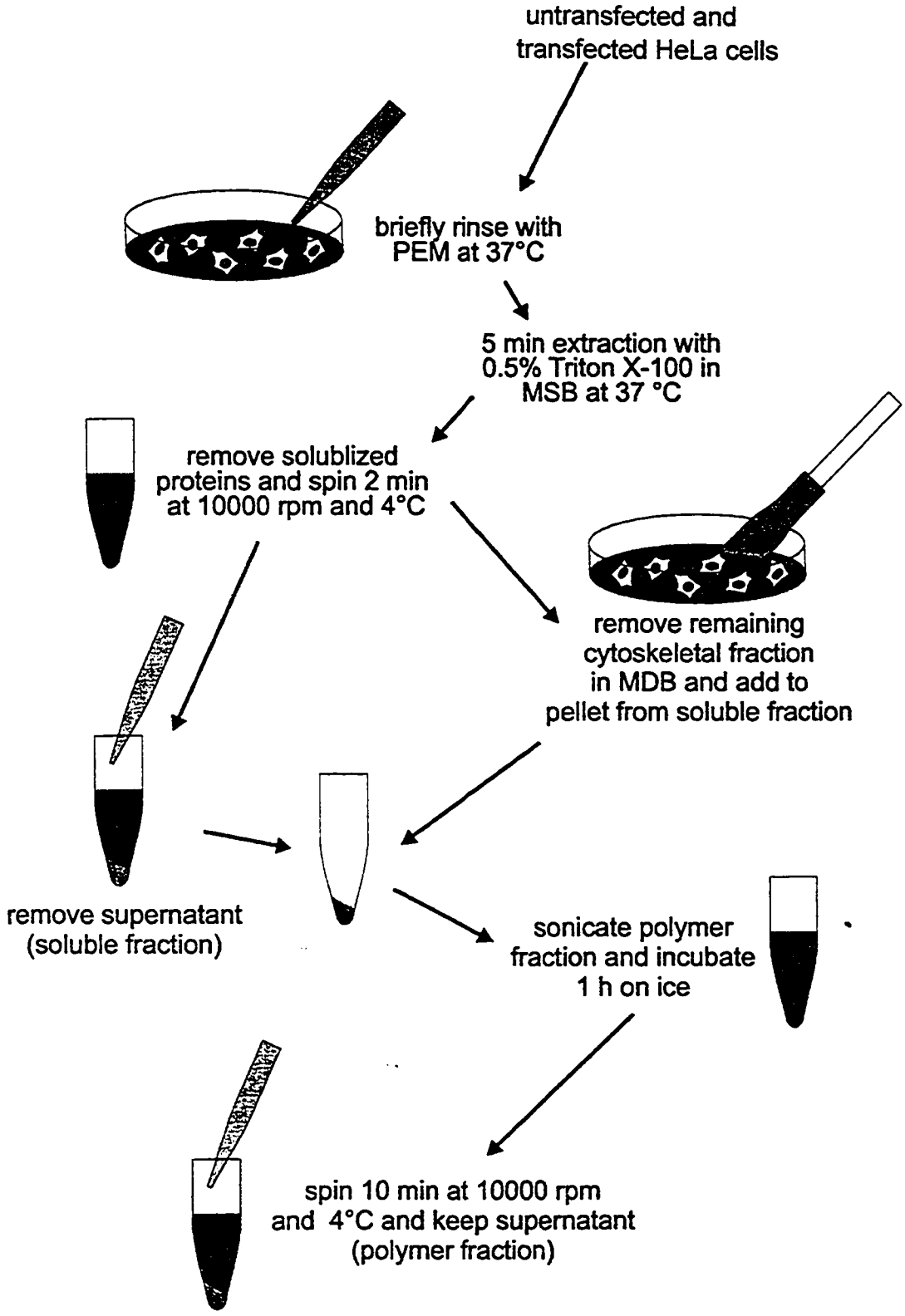
untransfected and
transfected HeLa cells
briefly rinse with
PEM at 37°C
5 min extraction with
0.5% Triton X-100 in
MSB at 37 °C
remove solublized
proteins and spin 2 min
at 10000 rpm and 4°C
remove remaining
cytoskeletal fraction
in MDB and add to
pellet from soluble fraction
remove supernatant
(soluble fraction)
sonicate polymer
fraction and incubate
1 h on ice
spin 10 min at 10000 rpm
and 4°C and keep supernatant
(polymer fraction)

H. SDS-PAGE and Western Blotting

Protein samples, diluted 1:1 in 2x sample buffer (Laemmli, 1970), as well as biotinylated SDS-PAGE broad range standard (BioRad) diluted 1:10 in 2x sample buffer and prestained broad range standard (BioRad) undiluted were boiled for 5 min, allowed to cool and were loaded onto 7.5 % and 10% polyacrylamide gels and separated using the BioRad minigel apparatus. Following separation, the proteins were electrotransferred ON onto nitrocellulose (NS)(Scleicher and Scheull) according to Towbin et al., 1979. The blots were rinsed in PBS and processed for western blotting. First, the blots were incubated at 4°C overnight in 5% (w/v) skim milk (Carnation) in PBS containing 0.05% Tween. This was followed by a 1 hr incubation in primary antibody diluted in 2% skim milk in PBS-Tween. The blots were washed 3x5 min in PBS-Tween. The blots incubated with the anti-EGFP rabbit polyclonal antibody conjugated to HRP antibody were then directly treated with the ECL+Plus Western blotting detection system (Amersham), whereas the blots incubated with the anti-MAP1A mouse monoclonal antibody were further incubated for 45 min in biotinylated horse anti-mouse polyclonal secondary antibody diluted in 2% skim milk followed by 3x5min washes in PBS-Tween. Next, these blots were incubated for 30 min in streptavidin-HRP (Amersham) diluted 1:5000 in PBS. In all blots, antibody binding was detected by enhanced chemiluminescence (ECL) (Amersha

using Hyperfilm–ECL (Amersham). Films were digitized at 400 dpi using a Hewlett-Packard 4c flatbed scanner. Digitized TIFF images were processed using Adobe Phtoshop v4.0 and Powerpoint 97 (Microsoft).

I. Fluorescence Microscopy

Cells grown on coverslips were briefly rinsed in PEM buffer and fixed by three different protocols:

1) Methanol fixation: cells were quickly immersed in MeOH at -20°C for 5 min. Coverslips were then re-equilibrated with 3x20 min PBS washes. This protocol was used for the anti-detyrosinated α-tubulin rabbit polyclonal antibody.

2) Extraction/fixation: first, cells were pre-extracted for 2min in 0.2% Triton X-100 in PEM buffer. Next, following a protocol from Falconer et al., 1992, the cells were simultaneously fixed and extracted for 10 min in 3.7% paraformaldehyde (v/v) (BDH), 0.25% glutaraldehyde (v/v) (JB EM Serviceces Inc.) and 0.5% Triton X-100 (v/v) in PEM buffer. Next, coverslips were washed 3x5 min in PBS wash, then 3x4 min with 1mg/ml $NaBH_4$ (BDH) in PBS, to reduce free aldehyde groups, and then rinsed again 3x5 min in PBS. This protocol was used for all the other antibodies used in this study.

3) Precipitation fixation (Stefanini et al., 1967): cells were incubated for 1 hour in the fixative solution containing 14% picric acid (Fisher), 4%

paraformaldehyde (JB EM Services Inc.) in 0.5M Na_2HPO_4, 0.5M NaH_2PO_4, pH 7.1 followed by a 3x5 min PBS wash, 5 min extraction with 0.5% Triton X-100 in PBS, and a final 3x5 min PBS wash. This protocol was used to determine the transfection efficiency.

Following fixation, cells were stained, according to the purpose of the investigation. Actin was stained with rhodamine-phalloidin (Molecular Probes Inc.) diluted 1:30. Nuclei were visualized with the DNA stain Hoechst (Calbiochem®) diluted 1:3000. Double immunofluorescence labelling was performed sequentially, in a humid chamber, at room temperature. Except for the anti-detyrosinated α-tubulin antibody incubation, which lasted 20 min, all antibody incubations were for 45 min with 3x5min PBS washes after each incubation. Cells were then mounted in Vectashield mounting medium (Vector Laboratories Inc) and visualized with a Zeiss Universal epi-fluorescence microscope equipped with a 50 W Hg burner. Images were digitally recorded with a Hamamatsu integrating CCD camera using Metamorph v 2.75 (Universal Imaging). All images were saved as TIFF files and were processed using Adobe Photoshop v. 4.0 and Powerpoint 97 (Microsoft).

J. Antibodies

5A6, a mouse monoclonal IgG specific for α-tubulin (Aitchison and Brown,

1986) was used for single immunolabelling at 1: 10,000.

YL 1/2, a rat monoclonal IgG which recognizes α-tubulin [clone YL 1/2 (Sera-Lab)] was used at 1:300 for double immunolabelling. **Anti-Acetylated α-Tubulin**, a mouse monoclonal IgG2b isotype [clone 6-11B-1 (Sigma)] was used at 1:500 for single immunolabelling.

Anti-Detyrosinated α-Tubulin, a rabbit polyclonal Ig (anti-E, Xiang and MacRae, 1995) provided by Dr.T.MacRae (Dalhousie University, NS) and used at 1:250 for single immunolabelling.

Anti-Vimentin, a mouse monoclonal IgG1 [clone V9 (Sigma) was diluted 1:2000 and used for single immunolabelling.

Anti-MAP1A, a mouse monoclonal IgG1isotype [clone HM-1 (Sigma)] was used at 1:1000 for immunoblotting.

Anti-EGFP, a rabbit polyclonal antibody [Living Colors® A.v. Peptide Antibody-HRP Conjugated (Clontech)] was used at 1:300 for immunoblotting.

Anti-6Myc Tag, a mouse monoclonal IgG (clone 9E10, Evan et al., 1985) provided by Dr. C. Garner (University of Alabama, AL) and used undiluted for single and double immunolabelling.

Anti-Mouse IgG

Donkey polyclonal IgG (H+L) conjugated to indocarbocyanine (CY3) (Jackson), crossadsorbed to rat and rabbit used at 1:400 for immunofluorescence microscopy.

Horse polyclonal IgG, biotinylated (Vector) and used at 1:1000 for immunoblotting. **Anti-Rat IgG**

Donkey polyclonal IgG (H+L) conjugated to carboxymethyl indocarbocyanine (CY2)(Jackson), cross-adsorbed to mouse and rabbit, used at 1:100 for immunofluorescence microscopy.

Anti-Rabbit IgG

Donkey polyclonal IgG (H+L) conjugated to indocarbocyanine (CY3)(Jackson) used at 1:400 for immunofluorescence microscopy.

III. RESULTS

A. MAP1A Is not Expressed in HeLa Cells

As an initial step in determining the localization of EGFP-LC2, the endogenous expression of MAP1A (heavy chain and LC2) in HeLa cells was investigated by western blotting and was compared with the expression of MAP1A in adult bovine brain, used as a positive control (**Fig. 10**). As expected, MAP1A was detected in adult bovine brain, as a single, strongh, immunoreactive band of high molecular weight (Langkopf et al, 1992). In contrast, MAP1A was not detected in untransfected HeLa cells and, therefore, this permited investigation of the exogenous expression of LC2 without the interference of endogenous MAP1A heavy and light chains. On the same blot (**Fig. 10**) several faint low molecular weight bands were stained non-specifically, as determined by immunoblotting controls in which the anti-MAP1A antibody was omitted (data not shown).

B. LC2 Is Expressed in Transiently Transfected HeLa Cells

To ensure that EGFP-LC2 was expressed correctly, its exogenous expression was analyzed by western blotting using anti-EGFP antibody and was compared with the expression of EGFP-tag alone, used as a positive control. Both EGFP-LC2 and EGFP protein were detected as

Figure 10: MAP1A is detected in S1, bovine brain extract (Obtained in our laboratory by Tania Villeneuve) but not in HeLa cell extract. 10 µg of whole HeLa cell extract and 10 µg S1, bovine brain extract respectively, were separated by SDS-PAGE on a 7.5% gel. MAP1A was immunodetected on western blots using anti-MAP1A mouse monoclonal antibody (clone HM-1). Molecular weight markers (MW) are in kDa.

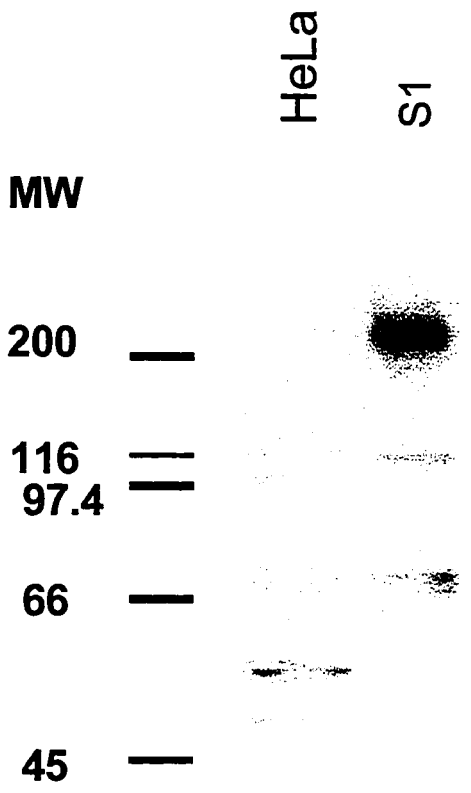
HeLa
S1
MW
200
116
97.4
66
45

Figure 11: Detection of EGFP-LC2 fusion protein and of the EGFP tag expressed in HeLa cells. 10µg of transfected whole cell extracts were separated by SDS-PAGE on a 10% gel. Both EGFP-LC2 and EGFP protein were immuno-detected on western blots using anti-EGFP rabbit polyclonal antibody conjugated to HRP. Molecular weight markers (MW) are in kDa.

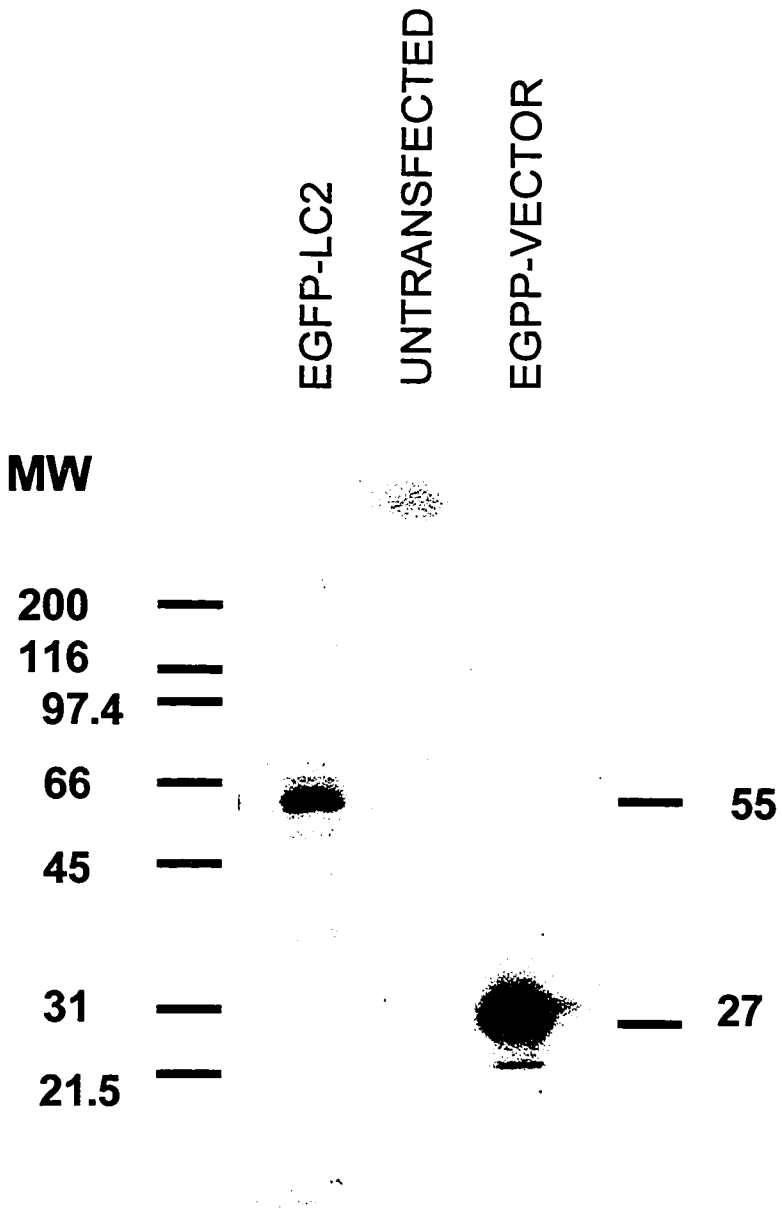
EGFP-LC2
UNTRANSFECTED
EGPP-VECTOR
MW
200
116
97.4
66
45
31
21.5
55
27

single bands that corresponded to their predicted molecular weights of 55kDa and 27kDa, respectively (**Fig. 11**). No signal was detected with the anti-EGFP antibody in untransfected HeLa cells, used as a negative control. Again, the faint bands migrating lower than EGFP-LC2 and EGFP protein respectively, were non-specifically stained.

C. LC2 Binds to MTs

C.1. *Fluorescence Microscopy*

To investigate if EGFP-LC2 binds to MTs, transiently transfected HeLa cells were simultaneously fixed and extracted and then observed by fluorescence microscopy. The MTs in the same cells were detected by immunolabelling with the 5A6 monoclonal anti-tubulin antibody (Aitchison and Brown, 1986). Expression of the EGFP-LC2 in HeLa cells revealed that it binds to MTs *in vivo* in the absence of the MAP1A heavy chain (**Fig. 12A'**, **B'**, **C'**, **D'**). In all transfected cells, EGFP-LC2 was detected as a bright staining in the nucleus as well. In 40% of the transfected cells, EGFP-LC2 was localized only in the nucleus and the cellular MT distribution was the same as in untransfected cells (data not shown); in 15% of transfected cells, EGFP-LC2 was observed as a dotted-pattern along the MTs (**Fig. 12A'**). In this case, EGFP-tagged LC2 was not only found to bind to MTs, but also induced a change in

Figure 12: Detection of different patterns of EGFP-LC2 localization in transfected HeLa cells (A', B', C', D') by fluorescence microscopy and immunofluorescence labelling of MTs using 5A6, a mouse monoclonal antibody specific for α-tubulin (A, B, C, D). In B the arrow points to some MTs with wavy appearance. Bar = 20 μm.

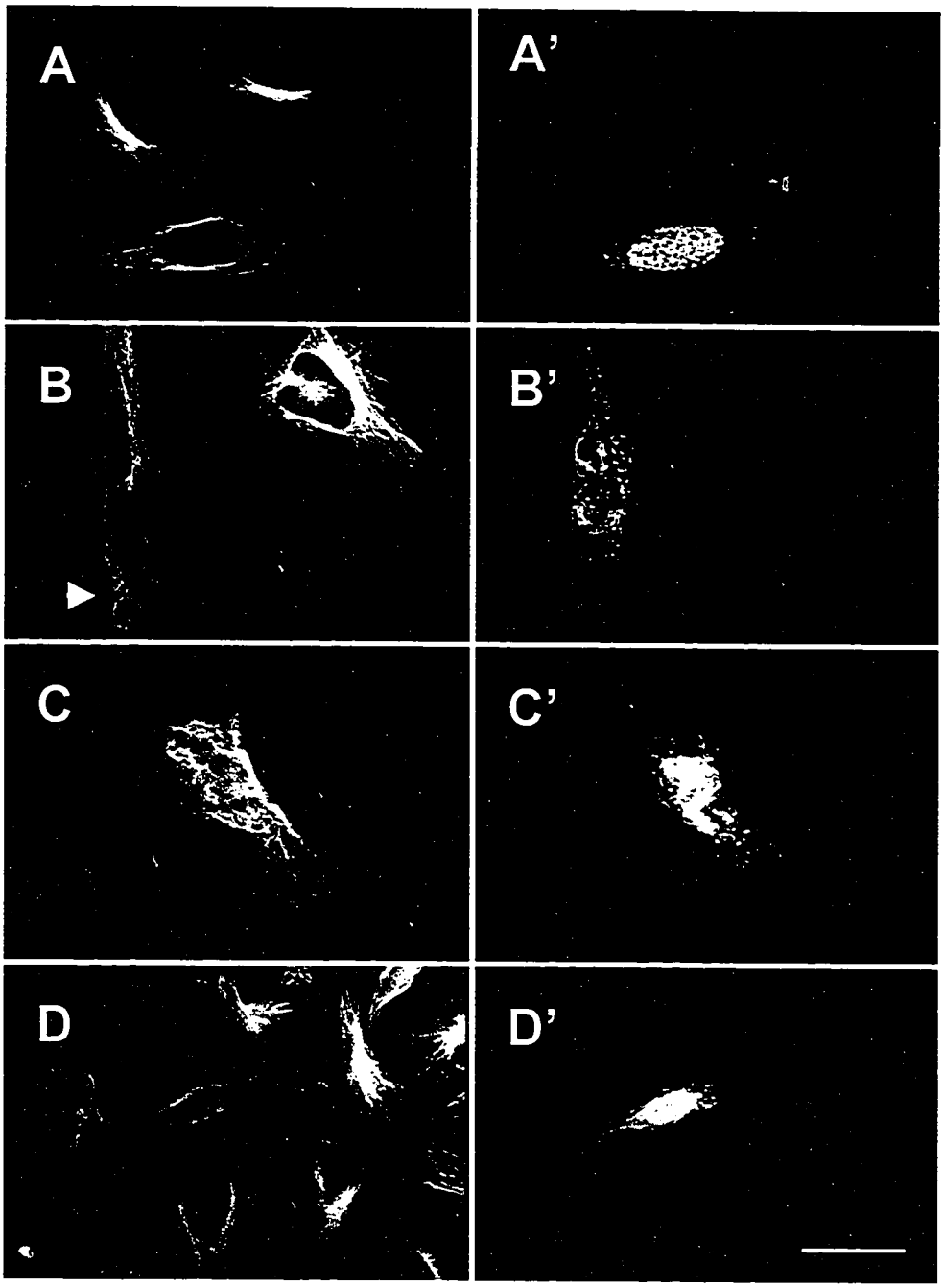
A
A'
B
B'
C
C'
D
D'

cellular MT distribution, with some MTs bundled around the nucleus (**Fig. 12A**). In 10% of transfected cells, EGFP-LC2 was found to bind MTs, both as dots and all along the MTs (**Fig. 12B'**). In this case, EGFP-tagged LC2, besides causing a change in cellular MT distribution, also induced a change in the morphology of some MTs, that assumed a wavy appearance (**Fig. 12B**). Finally, in 35% of transfected cells, EGFP- LC2 was found to bind all along MTs (**Fig.12 C'**, **D'**), and induced the wavy appearance of the majority of MTs (**Fig. 12C**, **D**). In most cases, the wavy MT bundles were present at higher density around the nucleus (**Fig.12 D**). These percentages are from counting a total of 300 cells from 6 different experiments.

C.2. *Biochemical Studies*

To verify that the EGFP-LC2 was indeed bound to MTs *in vivo*, MT proteins from EGFP-LC2 transfected HeLa cells as well as from EGFP-tag and EGFP-MAP2c transfected cells, used as controls, were extracted using a protocol in which the polymerized MT fraction was separately extracted from the soluble fraction (see **Fig. 9** Materials and Methods). Following protein separation by SDS-PAGE and Western blotting, using anti-EGFP antibody, both EGFP-LC2 and EGFP-MAP2c were detected only in the polymer fraction, whereas EGFP protein was

Figure 13: Detection of EGFP-LC2 (S1, P1), EGFP-MAP2c (S2, P2), and EGFP-tag (S3, P3), in transfected HeLa cells. 2μg of polymer (P1-P3) and 5μg of soluble (S1-S3) protein extracts were separated by SDS-PAGE on 10% polyacrylamde gels. EGFP was immunodetected by western blotting using anti-EGFP rabbit polyclonal antibody conjugated to HRP. Molecular weight markers (MW) are in kDa.

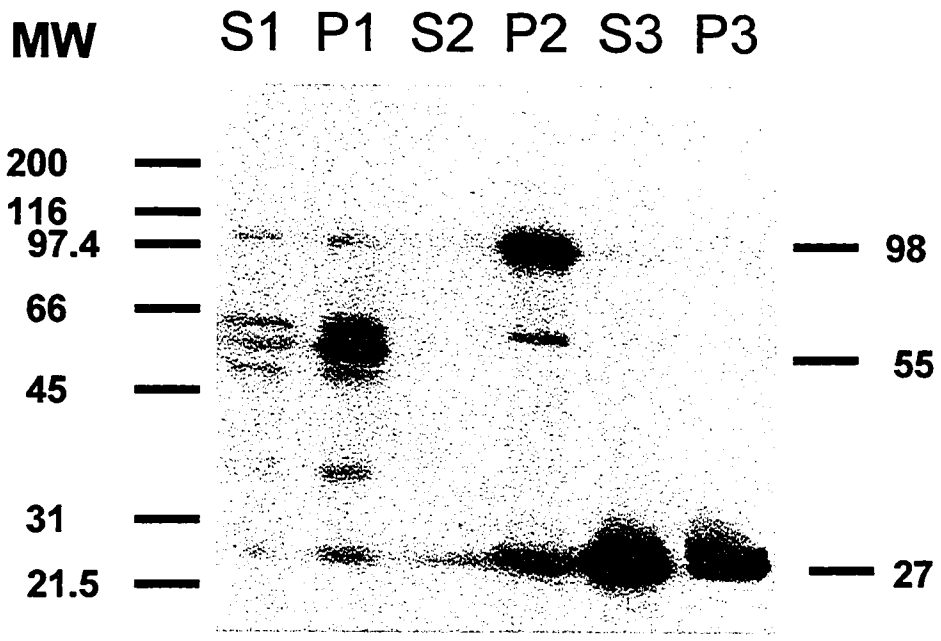
MW
S1
P1
S2
P2
S3
P3
200
116
97.4
66
45
31
21.5
98
55
27

detected both in the soluble and in the polymer fraction (**Fig. 13**). The detection of EGFP protein in the polymer fraction was the result of the presence of the tag protein in the nuclei of the EGFP transfected cells, and was not due to any associations with the polymerized MTs, as previously observed by fluorescence microscopy. The detection of EGFP-LC2 in the polymer fraction was partly due to its association with polymerized MTs, similar to that of EGFP-MAP2c, used as a positive control, and partly due to its presence in the in the nuclei of the transfected cells, similar to that of EGFP tag. In addition, several faint bands were the result of non-specific staining, as demonstrated by immunoblotting, in which the anti-EGFP antibody was omitted (data not shown). These results confirmed the previously observations by fluorescence microscopy.

D. The Effects of LC2 on the Cytoskeleton

D.1. *EGFP-LC2 Alters the MT Distribution*

To investigate the effects of LC2 on MTs, EGFP-LC2 transiently transfected HeLa cells (**Fig. 14 A"-D"**) were compared with untransfected HeLa cells (**Fig.14 A-B**), with cells transfected with the EGFP-vector alone (**Fig.14 A'-B'**), as well as with cells transfected with PGK-6myc1a (MAP1A heavy chain and light chain) (**Fig.15 A-B**) and

Figure 14: Phase contrast (A, A', A"), immunofluorescence labelling of MTs using 5A6, a mouse monoclonal antibody specific for α-tubulin (B, B', B'), and Hoechst staining of DNA (D, D', D") in untransfected (A-D), and transfected HeLa cells, with the vector alone (A'-D') and with the EGFP-LC2 expression construct (A"-D"). EGFP tag (C') and EGFP-LC2 (C") proteins were detected by fluorescence microscopy. Bar = 15μm.

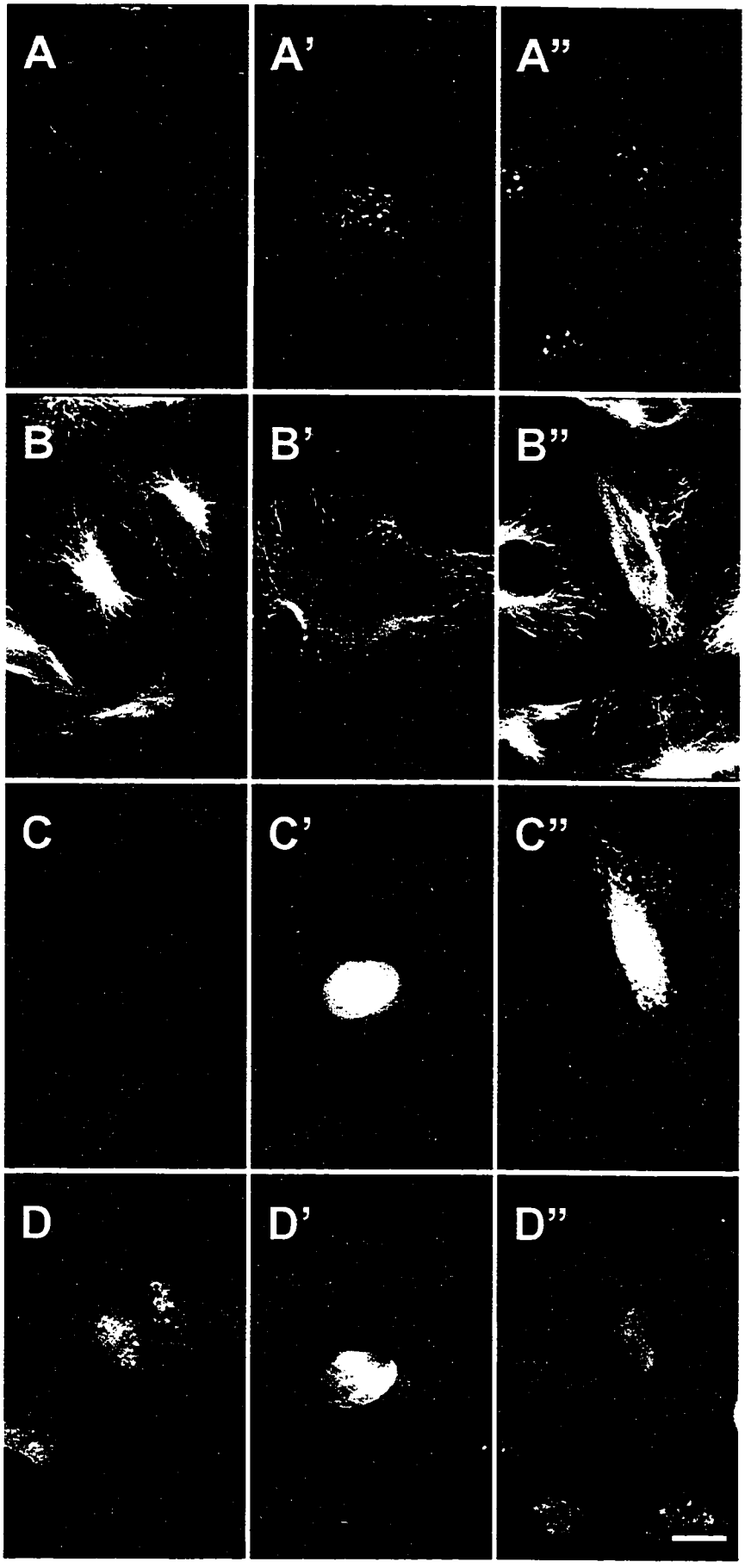
A
A'
A"
B
B'
B"
C
C'
C"
D
D'
D"

Figure 15: Phase contrast (A, A'), Hoechst staining of DNA (D, D') and double immunofluorescence labelling of MTs in cells transfected with PGK-6myc1a (A-D) and PGK-6myc N1a-4 (A'-D'). MTs were visualized using YL 1/2, a rat monoclonal antibody specific for α-tubulin (B, B'), whereas MAP1A (full length) and the longest MAP1a heavy chain fragment were visualized using 9E10, a mouse monoclonal antibody specific for the myc tag (C, C'). Bar=15μm.

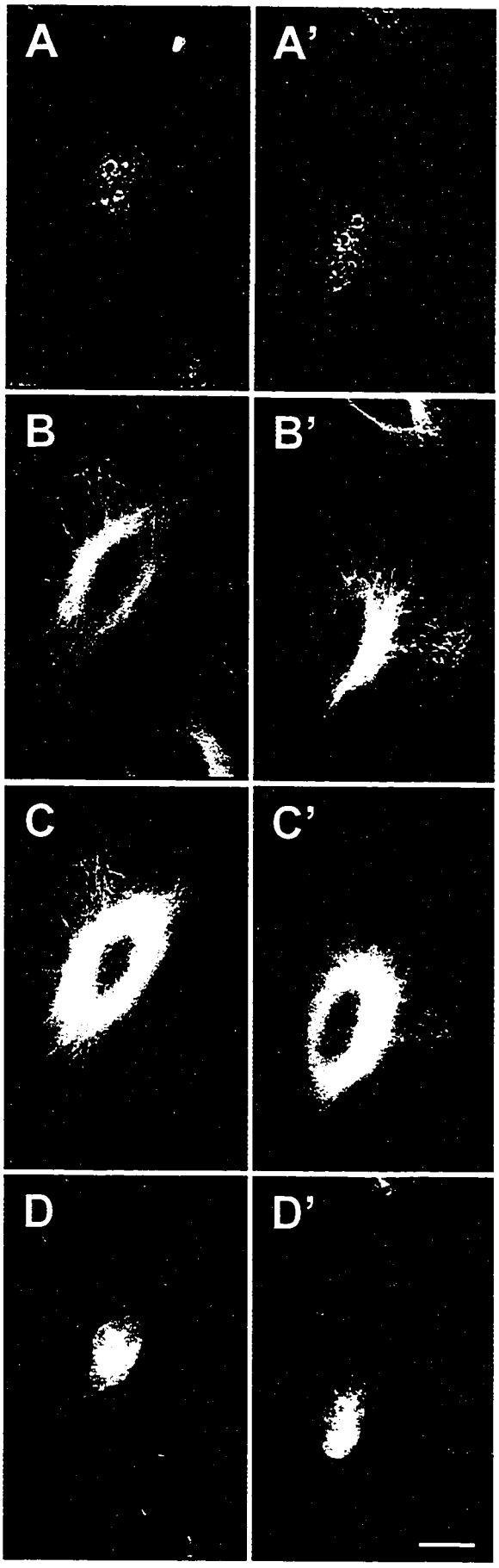
A
A'
B
B'
C
C'
D
D'

PGK-6mycN1a-4 (the longest MAP1A heavy chain fragment) (**Fig.15 A'-B'**). In untransfected HeLa cells, as a negative control, the MTs originated from one region, located near the nucleus, and extended to the cell periphery (**Fig.14 B**). EGFP tag protein not only does not colocalize with MTs (**Fig.14 C'**), but also does not have any effect on the MT distribution (Fig.14 **B'**). In contrast, as noted above, in 35% of EGFP-transfected HeLa cells, expression of LC2 in the absence of MAP1A heavy chain revealed that its colocalization with MTs *in vivo* also induced a change in cellular arrangement of most MTs, that assumed a wavy appearance with high density around the nucleus (**Fig.14 B"**; **Fig.12 C, D**). This altered MT arrangement was never observed in cells transfected with full-length MAP1A, consisting of heavy and light chain (PGK-6myc1a) (**Fig. 15 B**) or in cells transfected with any of the MAP1A heavy chain fragments (see, for example, the MT distribution in cells transfected with PGK-6mycN1-4, **Fig. 15B"**), in which the MT distribution was not altered as compared to that present in untransfected cells.

D.2. *EGFP-LC2 Induces a Change in Distribution of Vimentin*

To investigate if LC2 had any effect on vimentin, EGFP-LC2 transiently transfected HeLa cells (**Fig.16 A"-B"**) were compared with untransfected cells (**Fig.16 A-B**) and with cells transfected with the EGFP-vector alone (**Fig.16 A'-B'**). In untransfected HeLa cells (**Fig.16**

Figure 16: Immunofluorescence labelling of vimentin using anti-vimentin (clone 9), a mouse monoclonal antibody specific for vimentin (A, A', A") in untransfected (A-B), and transfected HeLa cells, with the EGFP-vector alone (A'-B') and with the EGFP-LC2 expression construct (A"-B"). EGFP tag (B') and EGFP-LC2 (B") proteins were detected by fluorescence microscopy. Bar = 20μm.

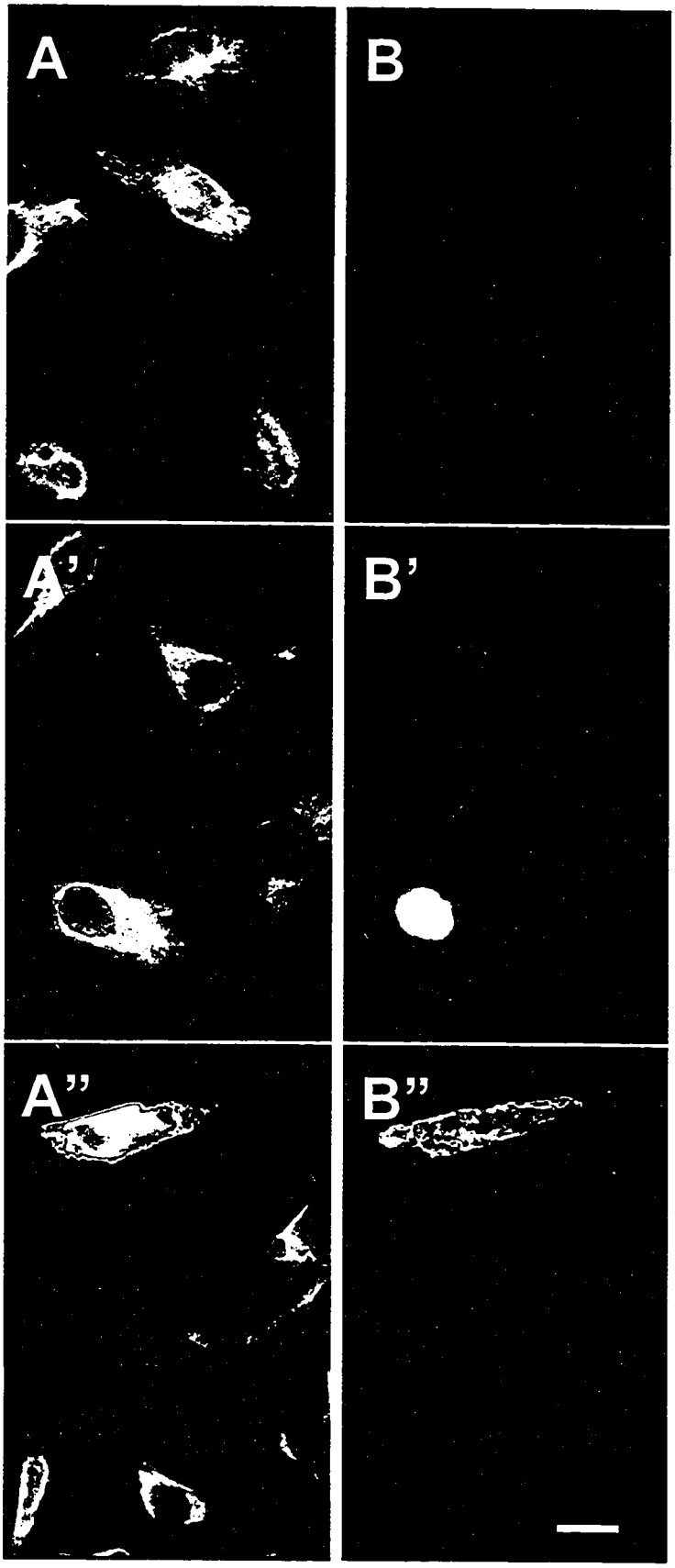
A
B
A'
B'
A''
B''

Figure 17: Immunofluorescence labelling of vimentin using anti-vimentin (clone 9), a mouse monoclonal antibody, specific for vimentin (A, red in merged image) in EGFP-LC2 transfected cells. EGFP-LC2 was detected by fluorescence microscopy (B, green in merged image). Merged image(C). Bar = 20μm.

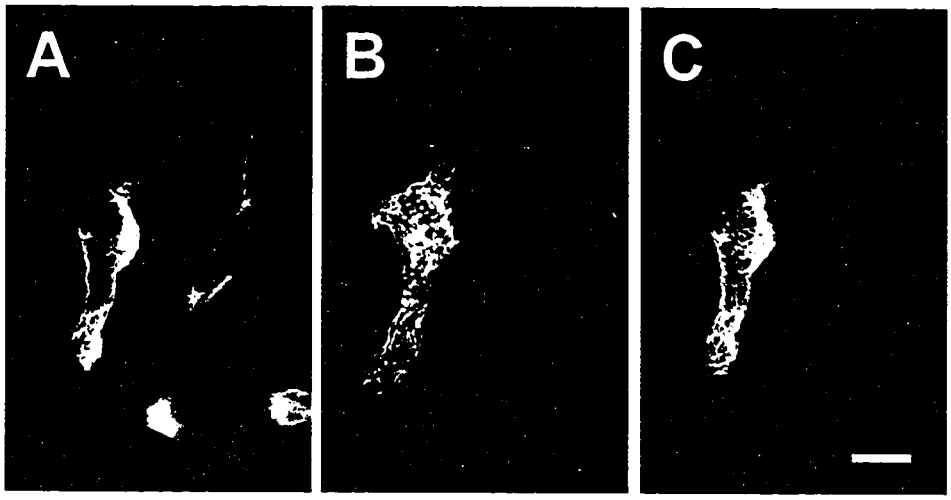
A
B
C

A), as a negative control, as well as in cells transfected with EGFP-vector alone (**Fig.16 A'**), the vimentin filaments filled the entire cytosol, presenting a pattern similar to that of MTs. In ~ 30% of EGFP-LC2 transfected HeLa cells, expression of LC2 induced a change in the distribution of intermediate filaments, that also presented a wavy pattern, forming bundles close to the nucleus (**Fig.16 A"**). The extent of colocalization of EGFP-LC2 with vimentin is shown in Fig. **17 C**. Overall, EGFP-LC2 did colocalize with the induced bundles of vimentin (**Fig. 17**, yellow in merged image, **C**). However, in regions of transfected cells where vimentin didn't form bundles (**Fig.17 A**, red in merged image, **C**) EGFP-LC2 did not colocalize with individual vimentin filaments (**Fig. 17 B**, green in merged image, **C**).

D.3. *EGFP-LC2 Does not Alter the Distribution of Actin*

In contrast to its effects on MT and IF distribution, EGFP-tagged LC2 did not appear to induce any modification in the distribution of rhodamine-phalloidin stained actin filament (**Fig.18**). In both transfected and untransfected cells (**Fig.18 A-B**), actin filaments were present as stress fibers and networks (**Fig.18 A**). In addition, LC2 did not colocalize with actin. To verify these results, transfected EGFP-LC2 cells were treated with the actin depolymerizing drug, cytochalasin B. Following this

Figure 18: Double fluorescence microscopy of rhodamine-phalloidin staining of actin (A, A') and of EGFP-LC2 (B, B') in transfected HeLa cells, untreated (A, B) and treated with the actin depolymerizing drug, cytochalasin B (A', B'). The arrow in A' indicates the transfected cell. Bar = 20 µm.

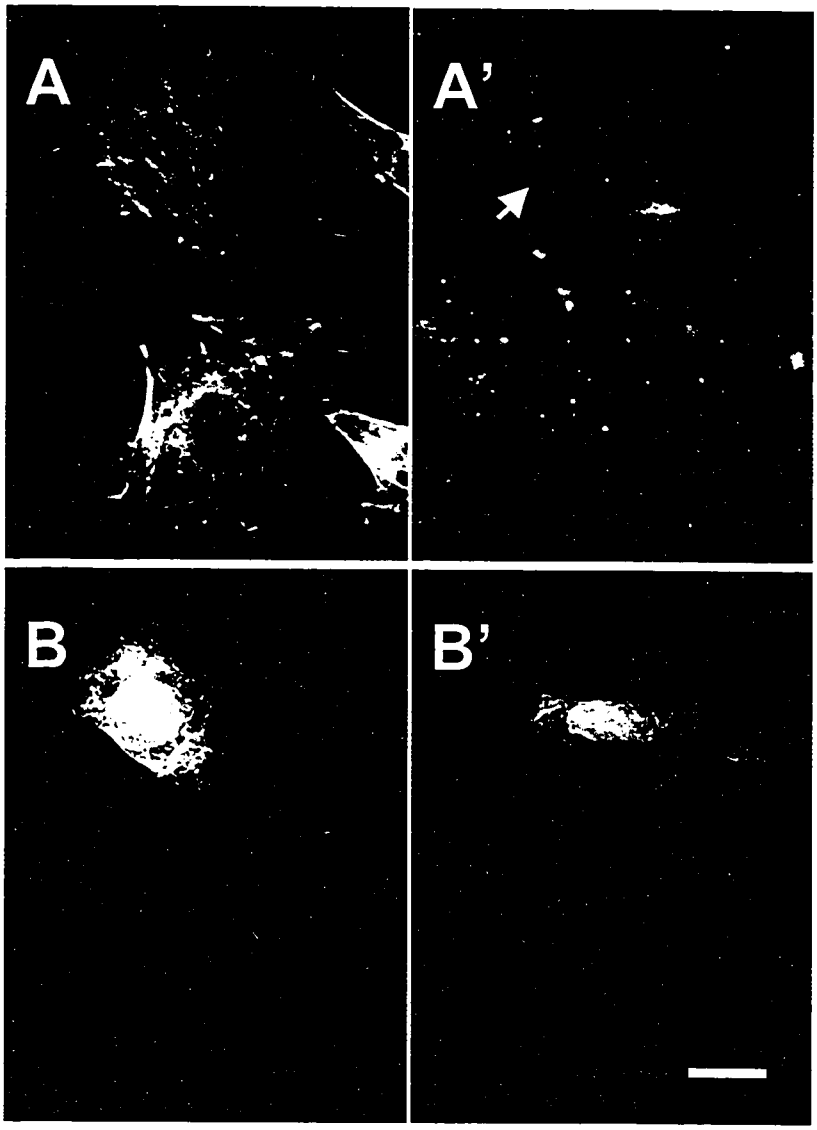
A
A'
B
B'

treatment, actin was depolymerized (**Fig.18 A'**), whereas EGFP-LC2 retained the filamentous wavy appearance (**Fig.18 B'**).

E. Investigation of the Effect of LC2 on MT Stabilization

E.1. *LC2 Stabilizes the MTs Against the Effects of Nocodazole*

To determine if by binding to MTs LC2 had any stabilizing effects, EGFP-LC2 transfected HeLa cells were treated with the MT depolymerizing drug, nocodazole (**Fig.19 A'-D'**). In untransfected cells in the population, nocodazole treatment caused the depolymerization of most MTs (**Fig.19 B'**). In contrast, the MTs were resistant to nocodazole in ~ 30% of the EGFP-LC2 transfected cells. In addition, the MTs again displayed the characteristic wavy pattern induced by LC2 (**Fig.19 B'**). These results demonstrated that LC2 by binding to MTs was capable of inducing MT stabilization.

E.2. *LC2 Stabilizes the MTs Against the Effects of Taxol*

To further verify the MT stabilizing effect of LC2, transfected cells were also treated with taxol (**Fig.19 A"-D"**). In untransfected cells in the population, taxol treatment induced multiple centrosome-independent MT bundles (**Fig.19 B"**) as compared with untreated HeLa cells in which the MTs extended from the centrozome in the whole cytoplasm to cell

Figure 19: Phase contrast (A, A', A"), immunofluorescence labelling of MTs using 5A6, a mouse monoclonal antibody specific for α-tubulin (B, B', B'), EGFP-LC2 fluorescence (C, C', C") and Hoechst staining of DNA (D, D', D") in transfected HeLa cells. Untreated cells (A-D), as a control, were compared with nocodazole (A'-D') and taxol (A"-D") treated cells. Bar = 20μm

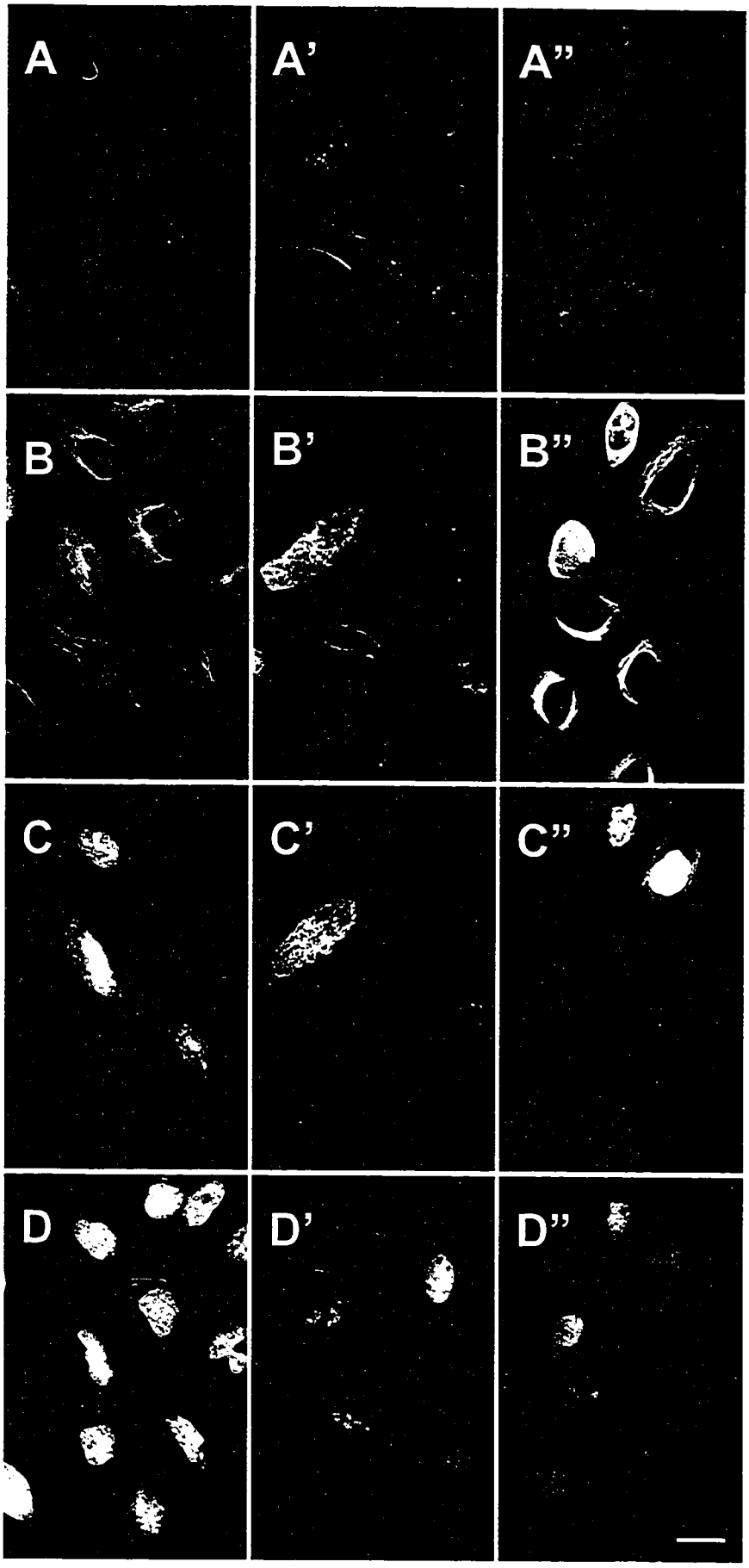
A
A'
A"
B
B'
B"
C
C'
C"
D
D'
D"

periphery (**Fig.19 B**). In living cells, by reducing the concentration of the soluble cytoplasmic pool of tubulin, taxol induces first the *de novo* polymerization and bundling of centrozome-independent MTs, and then the disassembly of the MTs originated in the MTOC (De Brabander et al. 1981; Horwitz et al., 1984; Caplow et al., 1994). In contrast, in ~30% of transfected cells, LC2 prevented the effect of taxol on MTs, that again displayed a wavy appearance (**Fig.19 B"**). These results suggested that LC2 by binding to MTs had a MT stabilizing effect and inhibited the MT-depolymerization induced by taxol.

E.3. *LC2 Colocalizes with a Subset of MTs that Contains Detyrosinated and Acetylated Tubulin in Their Structure*

To further verify the stabilizing effects of LC2 on MTs, the colocalization of EGFP-LC2 with stable MTs containing post-translationally modified tubulins was investigated by fluorescence microscopy (**Fig.20**). Acety-lation and detyrosination represent post-translational modifications of tubulin that have been shown to be biochemical markers of stable MTs with decreased dynamics (Laferrière et al., 1997, for review). The MTs were observed using either 5A6 monoclonal antibody that detected the total α-tubulin (**Fig.20 A**), or one of the following antibodies: clone 6-11B-1, a mouse monoclonal antibody

Figure 20: Immunofluorescence labelling of MTs using one of the antibodies: 5A6, a mouse monoclonal antibody specific for total α-tubulin (A); clone 6-11B-1, a mouse monoclonal anti-acetylated α-tubulin (A'); anti-E, a rabbit, polyclonal anti-detyrosinated α-tubulin (A"); EGFP-LC2 was detected by fluorescence microscopy (B, B', B"). Merged images (C, C', C"). Bar = 20μm.

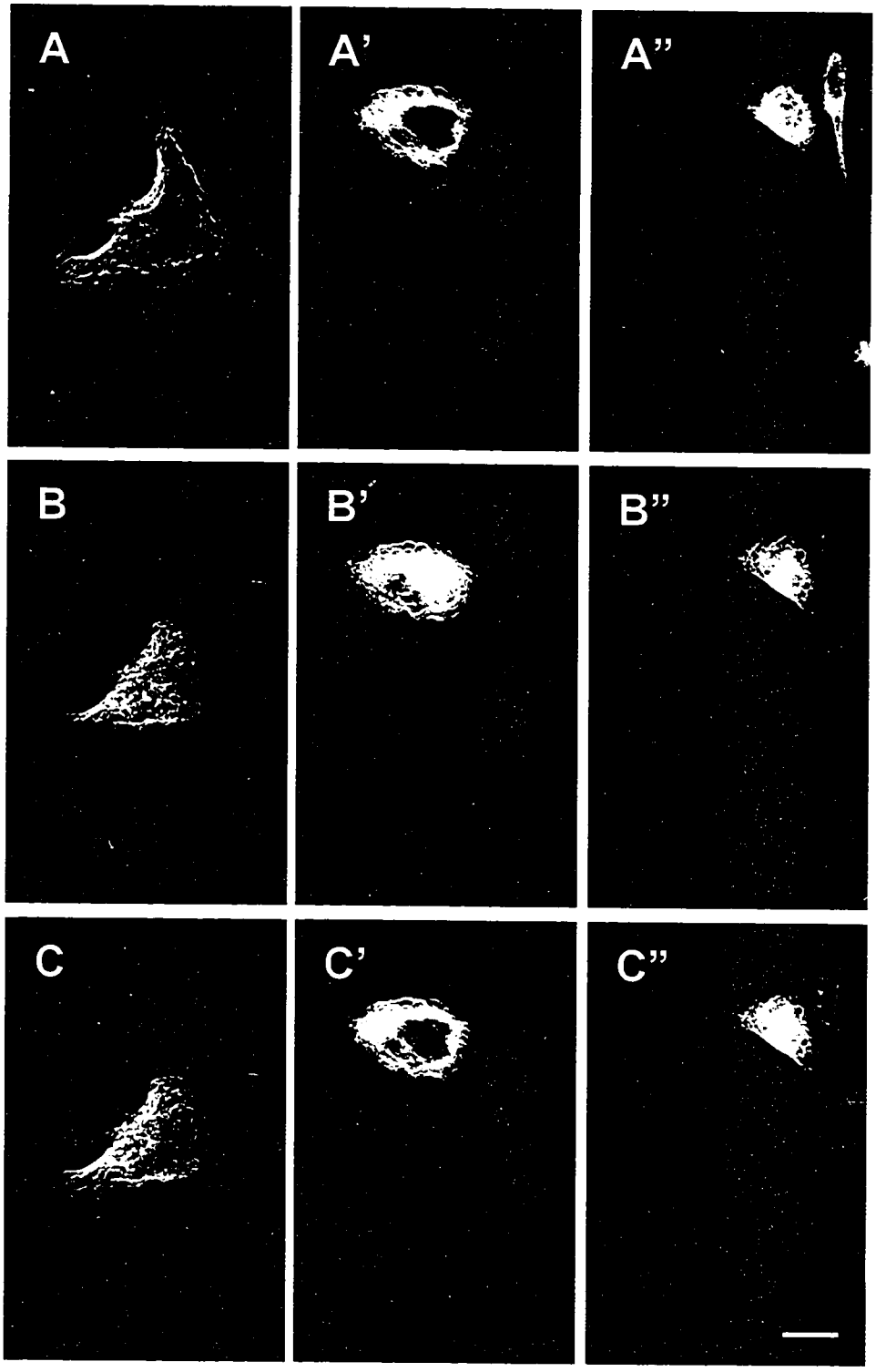
A
A'
A''
B
B'
B''
C
C'
C''

that detected only acetylated α-tubulin (**Fig.20 A'**); anti-E, a rabbit polyclonal antibody specific for detyrosinated α-tubulin (**Fig.20 A"**). In all cases, EGFP-LC2 colocalized

with the subset of MTs around the nucleus, where the MTs formed wavy bundles (yellow in the merged images, **Fig.20 C, C', C"**). These bundles were enriched in acetylated and detyrosinated tubulins and appeared brighter than the MTs in the untransfected cells in the population.

F. The Role of LC2 in MAP1A Heavy Chain-MT Interaction

The results presented above demonstrated, that in the absence of the MAP1A heavy chain, LC2 independently bound to MTs and altered their distribution and stability. In contrast, in cells expressing both MAP1A heavy chain and light chain, by transiently transfecting HeLa cells with PGK-6myc1a encoding the full-length MAP1A chain and light chain, MT distribution was not altered (**Fig.15 B**) and there was only a moderate effect on MT stability (see Vaillant et al., 1998).

To further investigate the role of LC2 in the MAP1A heavy chain – MTs interaction, HeLa cells were co-transfected with the EGFP-LC2 expression construct and with one of the following PGK-6myc MAP1A heavy chain fragment expression constructs: PGK-6mycN1a-2Δ BR (expressing AA 1-335 and 541-631 of MAP1A) and PGK- 6mycN1a-4

Figure 21: Immunodetection of the 6myc tagged MAP1A fragments 6mycN1a-2ΔBR (A, red in merged image C) 6mycN1a-4 (A'; red in merged image C') in co-transfected HeLa cells using 9E10, a mouse monoclonal antibody specific for the myc tag. EGFP-LC2 was detected by fluorescence microscopy (B, B' and green in the merged images C, C'). Bar = 20μm.

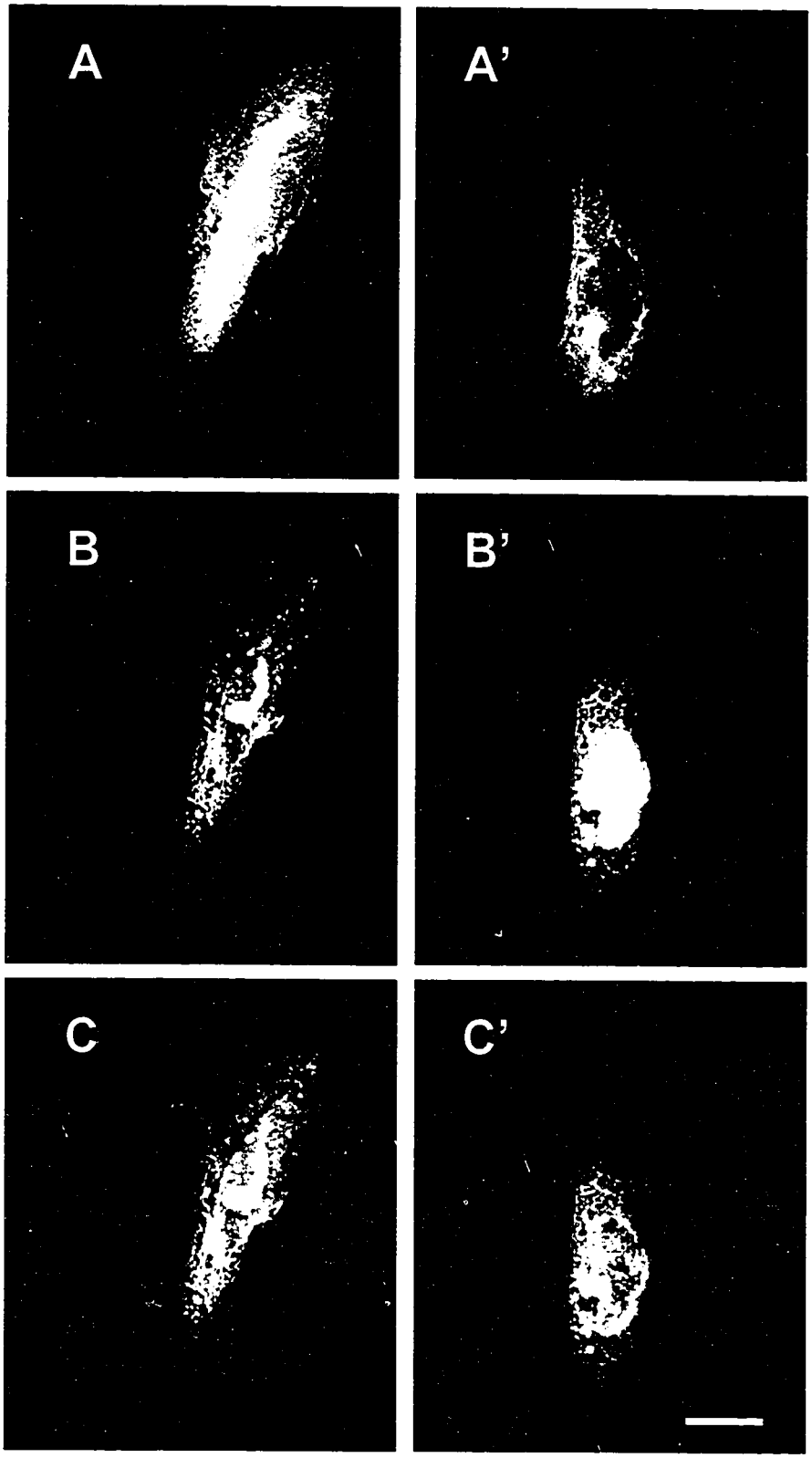
A
A'
B
B'
C
C'

(expressing AA 1-2016, the longest MAP1A heavy chain fragment). For each co-transfection, cells were fixed by extraction/fixation method (cells were first pre-extracted for 2 minutes in 2% Triton X-100 and then simultaneously extracted and fixed according to Falconer et al 1992) 48 hours and 72 hours after co-transfection. In each co-transfection experiment, there have been found a wide variety of patterns of expression both for EGFP-LC2 and for the 6myc tagged MAP1A fragments. The observations below are only of co-transfected cells in which the levels of expression of both EGFP-LC2 and the 6myc tagged MAP1A fragment appeared similar as judged from the intensity of staining.

In HeLa cells co-transfected with EGFP-LC2 and PGK- 6mycN1a-2Δ BR (**Fig. 21 A-C**), and in the cells co-transfected with EGFP-LC2 and PGK-6mycN1-4 (**Fig. 21 A'-C'**), 6mycN1a-2Δ BR (**Fig. 21 A**) and 6mycN1-4(**Fig. 21 A'**), respectively, presented a pattern similar to that of the MTs to which they bind. In both cases, EGFP-LC2 was found mostly around the nucleus, in a filamentous pattern **Fig. 21 B**, **B'**) co-localizing with 6mycN1a-2Δ BR (**Fig. 21** yellow in merged image **C**) and with 6mycN1-4 (**Fig. 21** yellow in merged image **C'**), respectively. These results suggest that MAP1A heavy chain has regulatory functions towards the LC2.

Figure 22: Detection of tubulin (YL 1/2, A, A') and of 6mycN1a-1 (9E10, B, B') in transfected HeLa cells by double immunofluorescence microscopy. Cells were fixed by extraction/fixation (A-B) or by precipitation (A'-B').
Bar =20µm.

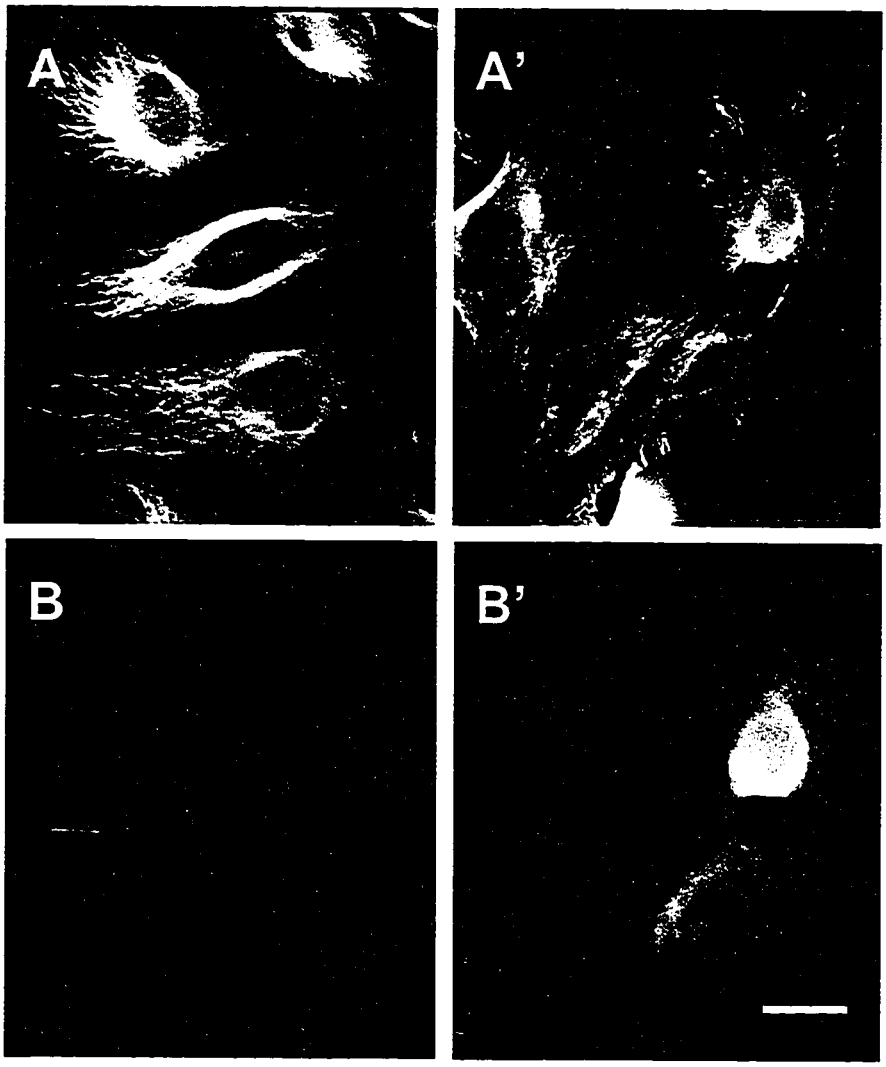
A
A'
B
B'

Figure 23: Immunodetection of 6mycN1a-1(9E10 mAb, A) and detection of EGFP-LC2 (B) in cotransfected HeLa cells by fluorescence microscopy. 6mycN1a-1 colocalizes with EGFP-LC2 previously attached to MTs (yellow in merged image C). Bar =20µm.

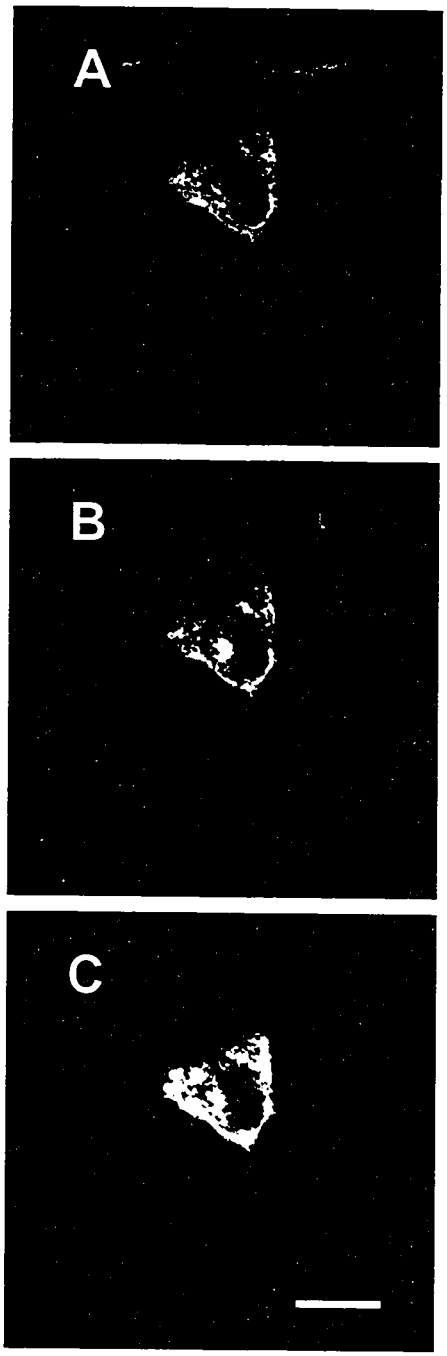
A
B
C

The possible association of 6mycN1a-1 with EGFP-LC2 was also investigated. It was previously determined in our laboratory (Vaillant et al., 1998) that 6mycN1a-1 does not bind to MTs and this was confirmed by results in the present study. **Figure 22 B** shows that 6mycN1a-1 was not detected in transfected HeLa cells which were fixed by extraction/fixation method, as above. To ensure that 6mycN1a-1 was indeed expressed, transfected cells were also fixed by the precipitation method (**Fig. 22 A'-B'**). Following this procedure, 6mycN1a-1 was observed as a diffuse cytoplasmic staining (**Fig. 22 B'**). However, when HeLa cells were co-transfected with 6mycN1a-1 and EGFP-LC2 and observed by fluorescence microscopy after extraction/fixation method (as above) (**Fig. 23 A-C**), 6mycN1a-1 was detected as a wavy pattern in the cytoplasm (**Fig. 23 A**) co-localized with EGFP-LC2 (**Fig. 23 B**), (**Fig. 23** yellow in merged image **C**). These results suggest that the binding site for LC2 of MAP1A heavy chain seems to be located between AA 1-281.

IV. DISCUSSION

To elucidate the functions of MAP1A, one of the most prominent MAPs in adult brain, previous *in vitro* studies have focused on the MAP1A protein complex as a whole (Shiomura and Hirokawa, 1987; Fuji et al., 1993; Pedrotti et al. 1993; Pedrotti and Islam, 1994; Pedrotti et al., 1994b; Pedrotti et al., 1996b) consisting of the heavy chain and its associated light chains (LC1, LC2, LC3). To gain some more insight into the MAP1A functions, additional studies (Cravchik et al., 1994; Vaillant et al., 1998) focused on the MAP1A heavy chain. To further characterize the functions of MAP1A in neurons, it was important to elucidate the functions of the MAP1A associated light chains. As it is encoded in the 3'end of the open reading frame of MAP1A (Langkopf et al., 1992; Fink et al., 1996), LC2 was the focus of the present study.

A. LC2 Binds to MTs and Alters Their Distribution

It was previously shown (Vaillant et al., 1998) both *in vivo* and *in vitro* that MAP1A heavy chain is able to bind to MTs, and that this association does not require the presence of LC2. In addition, in the same study the expression of MAP1A heavy chain in transfected cultured cells had no apparent effect on MT distribution. To determine if LC2 can also bind to MTs, preliminary studies in our laboratory (Vaillant,

1997) by immunofluorescence microscopy revealed that in P19 EC (embryonal carcinoma) and HeLa cells transiently transfected with PGK-6mycLC1, PGK-6mycLC2 or PGK-6mycLC3 expression constructs, the LCs could not be detected after extraction/fixation. However, the expression of myc-tagged LCs was confirmed both by immuno-fluorescence microscopy in cells prepared by the precipitation fixation and by Western blotting. In the present study, these results were verified and confirmed for the myc-tagged LC2 (data not shown).

It is possible that the failure of LC2 to bind to MTs in these studies is a consequence of a low affinity of association with MTs. This low binding affinity might be inherent to LC2 or it may be a consequence of the presence of the myc tag. The nature, the size and the position of the myc tag might interfere with the normal LC/MT interactions, so that the affinity of the LC2 for MTs is reduced. In either case the majority of the polypeptide would be easily removed by the detergent extraction. It is also possible that the PGK promoter only drives low levels of LC2 expression, and this in combination with inherent low affinity binding, may prevent detection.

In the present study, a new expression plasmid was constructed, the EGFP-LC2, in which the nature of the promoter and the nature and size of the tag were changed. With expression under the control of

the CMV promoter, the EGFP-LC2 fusion polypeptide was found by fluorescence microscopy to bind to MTs *in vivo*, in the absence of MAP1A heavy chain. These results demonstrated both that LC2 has its own MT binding site and that the association of LC2 with MTs does not require the presence of the MAP1A heavy chain. In addition, in transfected HeLa cells, EGFP-LC2 presented different patterns of localization that seems to be linked to different levels of expression. At low levels of expression, EGFP-LC2 was detected in the nucleus, but not associated with MTs of transfected cells. At higher levels of expression, EGFP-LC2 was detected not only in the nucleus, but also along the MTs, in a dotted pattern or continuos along the individual MTs. In these cells, EGFP-LC2 not only bound to MTs, but also induced a change in the cellular MT organization, with many MTs assuming a wavy appearance with high density in the nuclear region. The number of wavy MTs paralleled the increase in the co-localization of EGFP-LC2 with these MTs. The co-localization of EGFP-LC2 polypeptide with MTs and its effects on MT distribution seem unlikely to be due to the EGFP tag, as, by fluorescence microscopy, this tag was never found colocalized with MTs. Moreover, its expression had no effect on MT distribution in cells transfected with EGFP-vector when compared with untransfected cells.

The biochemical investigations confirmed these fluorescence

microscopy results. EGFP-LC2, similar to EGFP-MAP2c, was found only in the polymerized MT fraction, whereas EGFP, as expected, was found in the soluble fraction. However, the EGFP tag was also detected in the in the polymer fraction. This is due to the presence of the tag in the nucleus.

LC2 and LC1 are 55% identical, as deduced from comparison between MAP1A/LC2 and MAP1B/LC1 protein sequences (Műller et al., 1994, for review). Not surprisingly, the present results with LC2 were similar to that previously obtained for LC1, that was found to bind both *in vitro* (Zauner et al., 1992) and *in vivo* (Tőgel et al., 1998) to MTs. LC1 also induced a change in the distribution of MTs, that assumed a wavy appearance in cells (Tőgel et al., 1998), similar to that seen with LC2 in this study. Moreover, the wavy appearance of MTs was never observed in cells expressing the MAP1A heavy chain (Vaillant et al., 1998; present study, see **Fig. 15**) or MAP1B heavy chain alone (Tőgel et al., 1998) and, therefore, it seems to be a characteristic of LC2 and LC1, when they are bound to MTs in the absence of the corresponding heavy chains.

It is possible that the progressive LC2-induced change in MT distribution represents the consequences of an LC2-induced increase in MT stability (see further discussion below) that paralleled the increase in

LC2 expression. A similar progressive change in MT distribution that paralleled increased exogenous expression was seen in cultured cells transfected with the known MT stabilizer MAP2c (Weisshaar et al., 1992). In this case, at low MAP2c levels, MTs radiated from the MTOC, retaining their normal arrangement. As the MAP2c cellular concentration increased, MT were formed independently of the MTOC, then, they became bundled, and last, their orientation and position in the cell changed from radial to a circumferencial pattern (Weisshaar et al., 1992).

Another possible reason for the LC2-induced MT reorganization might be the result of a putative dimerizing property of LC2. In this respect, it was shown by immunoprecipitation that LC1 molecules can dimerize (Tőgel et al., 1998). These results were in agreement with previous biochemical investigations on MAP1A and MAP1B subunit stoichiometry (Schoenfeld et al., 1989; Pedrotti and Islam, 1994; Pedrotti et al., 1996a) demonstrating that the MAP1A and MAP1B heavy chains could bind more than one copy of each LC. Being structurally similar to LC1, it is possible that LC2 might dimerize as well and this might cross-link MTs and induce the change in MT morphology and distribution observed. For example, in some regions along the MTs, LC2 molecules may dimerize with LC2 molecules bound on neighboring MTs. In these

regions, MTs would be brought closer together than in regions where individual LC2 molecules are associated with the MTs. Consequently, this might generate the wavy MT appearance. Further studies are necessary to test the putative capacity of LC2 to dimerize.

B. LC2 Alters the Distribution of Vimentin

In this study, LC2 had an obvious effect on the distribution of vimentin, in transfected HeLa cells that showed a wavy pattern, similar to that of MTs. In addition, in merged images, LC2 partially colocalized with vimentin.

Previous studies, by solid-phase binding assays (Heimann et al., 1985; Furtner and Wiche, 1987) or by quick-freeze, deep-etch (QF-DE) electron microscopy of Purkinje cell dendrites (Shiomura and Hirokawa, 1987) revealed an association of MAP1A protein complex with neurofilaments (NFs). In these studies it was not determined if it was the MAP1A heavy chain or LC2 which accounted for the association with the NFs. To date, neither MAP1A heavy chain nor LC2 were separately investigated for their effect on NFs.

It is possible that LC2 binds directly to NFs and to vimentin IFs as well as to MTs. Vimentin is 65% identical in amino acid sequence to the light chain (NF-L) of NFs (Geisler et al., 1984). If LC2 does bind both

MTs and IFs, with or without dimerization as discussed above, it may cross-link the two cytoskeletal elements resulting in the wavy pattern that both display in transfected cells.

On the other hand, it is also possible that LC2 already bound to MTs, binds indirectly to vimentin and causes the wavy pattern. For example, it has been suggested that MAP1A protein complex might bind to plectin (Hermann and Wiche, 1987) and plectin has been shown to mediate MT-IF interactions (Svitkina et al., 1996).

A third possibility is that LC2 does not interact at all with IFs, but by altering MT stability indirectly affects MT-vimentin interactions. This study showed that MTs do become stable to anti-MT drugs and show increased acetylated and detyrosinated in LC2-transfected cells. Gundersen and coworkers (Gurland and Gundersen, 1995; Liao and Gundersen, 1998; Kreitzer et al., 1999) have shown that stable, detyrosinated MTs act to localize vimentin in 3T3 fibroblasts through a kinesin-dependent mechanism. Thus, LC2, by increasing the levels of detyrosination of MTs, may increase MT-IF interaction and lead to a redistribution of both.

Whatever the case might be, the present results demonstrate that LC2 can induce a change in vimentin intermediate filament distribution.

C. LC2 Does not Alter Actin Distribution

The present study showed that LC2 affected the distribution of MTs and IFs, but seemed to have no effect on the other major component of the cytoskeleton, the microfilaments. Previous biochemical studies demonstrated that MAP1A had both actin-binding (with both G- and F-actin) and actin-crosslinking activities (Fuji et al., 1993; Pedrotti et al., 1994b). However, in these studies it was not clear whether it was the MA1A heavy chain, or if it was one or more of the three associated LCs (LC1, LC2, LC3), which accounted for these activities. LC1 has been shown to contain separate C-terminus actin-binding and N-terminus MT-binding domains (Tőgel et al., 1998). LC2 is very similar in AA sequence (Lankopf et al., 1992; Fink et al., 1996) to LC1 and may also have separate binding domains. This raises the possibility that LC1 and LC2 are responsible for cross-linking MTs and actin filaments.

D. LC2 Has MT Stabilizing Activity

As was described in the Introduction, MAP1A and MAP1B are developmentally regulated, with MAP1B being expressed at its highest level early in brain development and with MAP1A appearing later in development (Műller et al., 1994; Hammarback, 1997, for reviews) and increasing to its highest levels in mature brain (Riederer and Matus,

1985; Matus, 1988; Garner et al., 1990; Fink et al., 1996). MAP1B has been shown to function in assembly of MTs in early neurite outgrowth (Ulloa, et al., for review, 1997) and it has been suggested that MAP1A may replace MAP1B functions, stabilizing MTs in mature neurons (Műller et al., 1994; Hammarback, 1997, for reviews). Support for this stabilizing function of MAP1A has come primarily from *in vitro* assembly studies (Pedrotti et al., 1993; Pedrotti and Islam, 1994) and from recent tubulin binding assays (Bonnet et al., 2001), showing that the binding affinity of MAP1A for tubulin increases with the increase in polyglutamylation of tubulin that occurs during neuronal maturation. Since the MAP1A complex was used in these studies, it was not clear whether the stabilizing/binding activity was due to the heavy chains, light chain(s), or a combination of these.

The present study demonstrated that besides affecting MT distribution, LC2 also affects MT stability. LC2 protects the induced MT bundles against the depolymerizing effect of nocodazole (**Fig. 19 A'-D'**) and of colchicine (data not shown). It also protected the MT bundles from the MT reorganizing actions of taxol. Similar results were previously obtained by nocodazole or taxol treatment of cells expressing exogenous LC1 (Tőgel et al., 1998). Consistent with the MT stabilizing action of LC2, the present study also showed an increase in the amount

of acetylated and detyrosinated α-tubulin in LC2 transfected cells.

In contrast to these effects of LC2, previous studies in our laboratory (Vaillant et al, 1998) demonstrated that the expression of the MAP1A protein complex, consisting of both heavy chain and LC2, as well as MAP1A heavy chain fragments, in transfected cells did not alter MT morphology and distribution in transfected cells, nor did they protect MTs against the effects of colchicine or taxol. However, in the same study (Vaillant et al., 1998), biochemical investigations on the effect of MAP1A protein complex on α-tubulin modifications demonstrated that, per molecule, MAP1A and MAP2c caused similar increases in acetylation and detyrosination relative to control cells, in contrast to MAP1A heavy chain fragments that had no effect. This suggested that the increase in the postranslational α-tubulin modifications seen with MAP1A complex was due to the presence of the LC2 in the protein complex (Vaillant et al., 1998).

Based on the results of the present and previous (Vaillant et al., 1998) studies, it can be concluded that LC2, when expressed by itself has strong MT stabilizing effects, whereas MAP1A heavy chain when expressed on its own seems to have no MT stabilizing effects. In addition, the MT stabilizing effect of LC2 is remarkably weakened in the presence of MAP1A heavy chain.

E. The LC2-MAP1A Heavy Chain-MT Interactions

LC2 not only binds to MTs as previously discussed, but also to the MAP1A heavy chain. Similarly, MAP1A heavy chain appears to have both MT-binding and LC-binding domains. When cells were co-transfected with EGFP-LC2 and one of the PKG-6myc MAP1A fragment expression constructs, EGFP-tagged LC2 was found to colocalize with all of the heavy chain fragments tested, included the N-terminus fragment lacking the MT binding domain. Early biochemical investigations showed the association of MAP1A heavy chain with LC2, as well as with LC1 and LC3 (Schoenfeld et al., 1989, Pedrotti and Islam, 1994).

The present study also identified the region of the MAP1A heavy chain that binds LC2. Earlier studies (Langkopf et al., 1992) by protein sequence analysis demonstrated that the N-terminus of MAP1B heavy chain exhibits 63% homology with the N-terminus of MAP1A heavy chain. As this region is highly conserved between the two polypeptides it has been suggested that it might have unknown but vital roles, among them a LC-binding activity (Langkopf et al., 1992; Fink et al., 1996). Both *in vivo* and *in vitro* studies have also demonstrated that the domain for the interaction with LC1 is localized within the first 508 AAs of the N-terminus of the MAP1B heavy chain (Tőgel et al., 1998). The present

study showed that in co-transfected cells both EGFP-LC2 and the 6mycN1a-1 fragment (AA 1s-281 from the N-terminus) of the MAP1A heavy chain were colocalized with MTs. Since the 6mycN1a-1 fragment alone does not bind to MTs this result suggests that it bound to MTs via LC2 and that the LC2-binding region of MAP1A heavy chain is localized in the N-terminus of the molecule too, between AA 1-281.

In addition, it is noteworthy that in co-transfected cells expressing both LC2 and 6mycN1a-1, LC2 and the MTs showed the characteristic wavy pattern. In contrast, in many co-transfected cells expressing LC2 and 6mycN1a-4 as well as in those expressing LC2 and 6mycN1a-2ΔBR (the MAP1A heavy chain fragment containing the MT-binding domain that consists only of the two flanking regions), LC2 did not show the wavy pattern and the overall MT organization appeared as in untransfected cells. Previous studies (Vaillant et al., 1998) also demonstrated that in cells transfected with the PGK-6mycN1a, vector encoding the full-length MAP1A, and consequently expressing both the MAP1A heavy chain and light chain, MT organization was not altered. These results suggest that the interaction of the heavy chain with both LC2 and with MTs modulated the effects of LC2 in stabilizing and reorganizing MTs.

Similar results were obtained in cells co-expressing LC1 and

the full length MAP1B heavy chain in which neither the LC1 nor the MTs presented the wavy pattern (Tőgel et al., 1998). Consequently, it has been proposed that MAP1B heavy chain controls the activity of LC1 and represents the regulatory subunit of the MAP1B complex (Tögel et al., 1998). Similarly, based on present and previous (Vaillant et al., 1998) results, it can be hypothesized that MAP1A heavy chain represents the regulatory subunit of the MAP1A protein complex and controls LC2 activity.

F. Concluding Remarks

Previous studies (Vaillant et al., 1998) demonstrated that MAP1A heavy chain can bind to MTs on its own. The present study demonstrated for the first time, that LC2, similar to LC1 (Tőgel et al., 1998), also binds to MTs on its own. In neurons, however, where both MAP1A heavy chain and its associated LCs (LC1, LC2, LC3) are normally expressed, the effects of MAP1A on MTs and other components of the cytoskeleton represents the results of the MAP1A heavy chain-LCs interactions and, probably, of the LC-LC interactions as well.

The present study offered the first information regarding the MAP1A heavy chain-LC2 interactions. In the future, biochemical

investigation of the association of LC2 with each of the MAP1A heavy chain fragments could provide a better understanding of the LC2-MAP1A heavy chain interactions and, consequently, of the interaction of the MAP1A complex with MTs. Even though LC2 presents high sequence similarity with LC1 and may have similar functions, it might also exhibit different functions. LC3 may also have different functions. LC3 is encoded by a separate gene (Mann and Hammarback, 1994) and its expression increases throughout neuronal differentiation (Mann and Hammarback, 1996; Vaillant, 1997) in parallel with MAP1A expression and with MT stability.

In order to better understand the function of MAP1A in neurons, it is important that future work determine the capacity of LC2 as well as of LC3 to dimerize. Equally important will be to determine if the different types of LCs can associate with each other and what effects such associations might have on MAP1A binding and on MT dynamics. Finally, it will be important to determine how the MAP1A complex interacts with other cytoskeletal proteins and what roles such interactions play in neuronal functions.

In conclusion, the elucidation of the functions of MAP1A associated light chains will provide a better understanding of neuronal functions. On the one hand, as already mentioned, the increasing MAP1A expression

in developing brain parallels an increase in MT stability. Therefore, it has been suggested that MAP1A indirectly, by stabilizing MTs in mature neurons, plays a role in maintaining neuronal morphology (Műller et al., 1994, for review) and is involved in all the neuronal processes that requiere stable MTs. For example, in neurons, stable MTs are implicated in vesicle transport, synaptic transmission (Wooten et al. , 1975; Knowles et al, 1996; Carson et al., 1997) and synaptic memory (Kohrmann et al., 1999). In addition, in adult brain, τ protein might be progressively replaced by MAP1A, that consequently could confer new structural and functional properties to MTs, such as a the change in spacing between MTs or the ability to interact with different set of axonal proteins (Bonnet et al., 2001). On the other hand, MAP1A is also expressed in regions of the brain where neuronal growth persists, such as the optic (McKerrracher et al., 1989) and the olfactory nerves (Schonefeld et al., 1989), suggesting that, by rendering MTs moderately dynamic, MAP1A is associated with neurite outgrowth and plasticity.

REFERENCES:

Addison, C.J. 1997. Microtubule-associated protein 2 (MAP2) expression in transiently and stably transfected P19 embryonal carcinoma cells. *M.Sc. thesis,* Ottawa, Canada.

Aitchison, W.A. and D.L.Brown. 1986. Duplication of the flagellar apparatus and cytoskeletal microtubule system in the alga *Polytomella. Cell Motil. Cytoskeleton* **6:** 122-127.

Barlow, S., Gonzalez-Garay, M.L., West, R.R., Olmsted, J.B., and F.Cabral. 1994. Stable expression of heterologous micro-tubule-associated proteins (MAPs) in chinese hamster ovary cells: evidence for differing roles of MAPs in microtubule organization. *J.Cell Biol.* **126:** 1017-1029.

Bonnet, C., Boucher, D., Lazereg, S., Pedrotti, B., Islam, K., Denoulet, P., and J.C.Larcher. 2001. Differential binding regulation of micro-tubule-associated proteins MAP1A, MAP1B, and MAP2 by tubulin polygutamylation. *J.Biol.Chem.* **276:** 12839-12848.

Brugg, B., Reddy, D., and A.Matus. 1993. Attenuation of microtubule-associated protein 1B expression by antisense oligodeoxynucleotides inhibits initiation of neurite outgrowth.*Neurosci.* **52:** 489-496.

Carson, J.H., Worboys, K., Ainger, K., and E., Barbarese. 1997. Translocation of myelin basic protein mRNA in oligodendrocytes requires microtubules and kinesin. *Cell Motil. Cytoskeleton* **38:** 318-328.

Caplow, M., Shanks, J., and R.Ruhlen. 1994. How taxol modulates microtubule disassembly. *J.Biol.Chem.* **269:** 23399-23402.

Cassimeris, L. 1993. Regulation of microtublue dynamic. instability. *Cell Motil. Cytoskeleton* **26:** 275-281.

Chapin, S.J., and J.C. Bulinski. 1992. Microtubule stabilization by assembly-promoting microtubule-associated proteins: a repeat performance. *Cell Motil.Cytoskeleton* **23:** 236-243.

Cravchik, A., Reddy, D., and A.Matus.1994. Identification of a novel microtubule-binding domain in microtubule-associated. protein 1A (MAP1A). *J.Cell Sci.* **107:** 661-672

Collins, C.A., and R.B. Vallee. 1987. Temperature-dependent reversible assembly of taxol-treated microtubules. *J.Cell. Biol.* **105:** 2847-2854.

De Brabander, M., Geunes, G., Nuydens, R., Willebrords, R., and J.De Mey. 1981. Taxol induces the assembly of free microtubules in living cells and blocks the organizing capacity of the centrosome and kinetochores. *Proc.Natl.Acad.Sci.U.S.A.* **78:** 5608-5612.

Doll, T., Meichsner, M., Riederer, B.M., Honegger, P., and A.Matus. 1993. An isoform of microtubule-associated protein 2 (MAP2) containing four repeats of the tubulin binding motif. *J.Cell Sci.* **106:** 633-640.

Drubin, D.G., and M.W. Kirschner. 1985. Tau protein function in living cells. *J.Cell Biol.* **103:** 2739-2746.

Edelman, W., Zervas, M., Costello, P., Roback, L., Pischer, I., Hammarback, J.A., Cowan, N., Davies, P., Wainer, B., and R.Kucherlabati.1996. Nueuronal abnormalities in microtubule-associated protein 1B mutant mice. *Proc.Natl.Acad. Sci.*USA. **93:** 1270-1275.

Evan, G.I., Lewis, G.K., Ramsay, G., and J.M. Bishop. 1985. Isolation of monoclonal antibodies specific for the human c-myc proto-oncogene product. *Mol.Cell Biol.* **5:** 3610-3616.

Falconer, M.M., Echeverri, C.J., and D.L. Brown. 1992. Differential sorting of beta-tubulin isotypes into colchicine-stable microtubules during neuronal and muscle differentiation of embryonal carcinoma cells. *Cell Motil. Cytoskeleton* **21:** 313-325.

Fink, J.K., Jones, S.M., Esposito, C., and J.Wilowski. 1996. Human microtubule-associated protein 1A (MAP1A) gene:

genomic organization, cDNA sequence, and developmental- and tissue- specific expression. *Genomics* **35:** 577-585.

Fuji, T., Watanabe, M., Ogoma, Y., Kondo, Y., and T.Arai. 1993. Microtubule-associated proteins, MAP1A and MAP1B, interact with F-actin *in vitro. J. Biochem.* **114:** 827-829.

Fukuyama, R., and S.I. Rapoport. 1995. Brain-specific expression of human microtubule-associated protein 1A (MAP1A) gene and it is assignment to human chromosome 15. *J.Neurosci. Res.* **40:** 820-825.

Furtner, R., and G.Wiche. 1987. Binding specificities of purified porcine brain alpha- and beta- tubulin subunits and of microtubule-associated proteins 1 and 2 examined by electron microscopy and solid-phase assays. *Eur. J.Cell Biol.* **45:** 1-8.

Garner, C.C., Garner, A., Huber, G., Kozak, C., and A.Matus. 1990. Molecular cloning of microtubule-associated protein 5 (MAP1B): identification of distinct genes and their differential expression in developing brain. *J.Neurochem.***55:** 146-154.

Geisler, N., Fischer, S., Vandekerckhove, J., Plessmann, U., and K. Weber. 1984. Hybrid character of a large neurofilament protein (NF-M): intermediate filament type sequence followed by a long and acidic carboxy-terminal extension. *EMBO J.* **3:** 2701-2706.

Goedert, M., Baur, C.P., Ahringer, H., Jakes, R., Hasegawa, M., Spillantini, M.G., Smith, M.J., and F.Hill. 1996. PTL-1, a microtubule-associated protein with tau-like repeats from the nematode *Caenrhabiditis elegans. J. Cell Sci.* **109:** 2661-2672.

Gonzalez-Billault, C., Demandt, E., Wandosell, F., Torres, M., Bonaldo, P., Stoykova, A., Chowdhury, K., Gruss, P., Avila, J., and M. Sanchez. 2000. Prenatal lethality of microtubule-assoicated protein 1B deficient mice expressing alternative isoforms of the protein at low levels. *Mol. Cell. Neurosci.* **16:** 408-421.

Gonzalez-Billault, C., Avila, J., and A.Cáceres. 2001. Evidence for the role of MAP1B in axon formation. *Moll. Biol. Cell* **12:** 2087-2098.

Gurland, G. and G.G.Gundersen. 1995. Stable, detyrosinated microtubules function to localize vimentin intermediate filaments in fibroblasts. *J. Cell Biol.* **131:** 1275-1290.

Gustake, N., Trinczek, B., Biernat, J., Mandelkow, E.-M., and E.Mandelkow. 1994. Domains of τ protein and interactions with microtubules. *Biochemistry* **33:** 9511-9522.

Hammarback, J.A., Obar, R.A., Hughes, S.M., and R.B.Vallee. 1991. MAP1B is encoded as a polyprotein that is processed to form a complex N-terminal microtubule-binding domain.

Neuron **7:** 129-139.

Hammarback, J. A. 1997. Distinct structural features of the microtubule associated protein 1 family: MAP1A and MAP1B. MAP1 structure. In: Brain microtubule associated proteins. Modifications in Disease. Eds. , Avila, J., Brandt, R., and Kosik, K.S., pp. 3-16. Harwood Academic Publishers, Canada.

Hanahan, D. 1983. Studies of transformation of *Escherichia coli* with plasmids. *J. Mol. Biol.* **166:** 557-580.

Heimann, F, Shelanski, M.L., and R.K.Liem. 1985. Microtubule-assoicated proteins bind specifically to the 70-kDa neurofilament protein. *J.Biol. Chem.* **260:** 12160-12166.

Herrmann, H., and G. Wiche. 1987. Plectin and IFAP-300 kDa are homologous proteins binding to microtubule-associated proteins 1 and 2 and to the 240 kDa subunit of spectrin. *J.Biol. Chem.* **262:** 1320-1325.

Horwitz, S.B., Schiff, P.B., Parness, J., Manfredi, J.J., Mellado, W., and S.N. Roy. 1986. In: The cytoskeleton. A target for toxic agents. eds. Clarkson, T.W., Sager, P.R., and T.L.M.Syversen, pp.53-65. Plenum Press, NY.

Joshi, H.C., and D.W. Cleaveland. 1989. Differential utilization of β-tubulin isotypes in differentiating neurites. *J.Cell Biol.* **109:** 663-673.

Kindler, S., Shwanke, B., Schulz, and C.C.Garner. 1990. Complete cDNA sequence encoding rat high and low molecular weight MAP2. *Nucleic Acids Res.* **18:** 2882.

Knowles, R.B., Sabry, J.H., Martone, M.E., Deerinck, T.J., Ellisman, M. H., Bassell, G.J., and K.S. Kosik. 1996. Translocation of RNA granules in living neurons. *J. Neurosci.* **16:** 7812-7820.

Kohrmann, M., Luo, M., Kaether, C., DesGroseillers, L., Dotti, C.G., and M.A. Kiebler. Microtubule-dependent recruitment of Staufen-green fluorescent protein into large RNA-containing granules and subsequent dendritic transport in living hippocampal neurons. *Mol.Biol.Cell* **10:** 2945-2953.

Kreitzer, G., Liao, G., and G.G.Gundersen. 1999. Detyrosination of tubulin regulates the interaction of intermediate filaments with microtubules in vivo via a kinesin-dependent mechanism. *Mol. Bol. Cell* **10:** 1105-1118.

Kuznetsov, S.A., Rodionov, I.V., Nadezhdina, E.S., Murphy, D.B., and V.I.Gefand. 1986. Identification of a 34-kD polypeptide as a light chain of microtubule-associated protein-1 (MAP-1) and its association with a MAP-1 peptide that binds to microtubules. *J.Cell Biol.* **102:** 1060-1066.

Kuznetsov, S.A., and V.I. Gelfand. 1987.18 kDa microtubule-associated protein: identification as a new light chain (LC3) of microtubule–associated protein 1 (MAP-1). *FEBS (Fed. Eur. Biochem. Soc.) Lett* **212:**145-148.

Laemmli, U.K. 1970. Cleavage of structural proteins during the assembly of the head of bacteriophage T4. *Nature* **227:** 680-685.

Laferrière, N.B., MacRae, T., and D.L.Brown. 1997. Tubulin synthesis and assembly in differentiating neurons. *Biochem. Cell. Biol.* **75:** 103-117.

Langkopf, A., Hammarback, J.A., Müller, R., Vallee, R.B., and C. Garner. 1992. Microtubule-associated protein 1A and LC2. Two proteins encoded in one messenger RNA. *J.Biol.Chem.* **267:** 16561-16566.

Liao, G. and G.G. Gundersen. 1998. Kinesin is a candidate for cross-bridging microtubules and intermediate filaments. *J.Biol.Chem.* **273:** 9797-9803.

Ludueña, R.F., 1998. Multiple forms of tubulin; different gene products and covalent modifications. *Int. Rev. Cytol.* 178: 207-275.

Maccini, R.B., and V.Cambiazo. 1995. Role of microtubule-associated proteins in the control of microtubule assembly. *Physiol.Rev.* **75:** 835-864.

Mann, S.S., and J.A., Hammarback. 1994. Molecular characterization of light chain 3. A microtubule binding subunit of MAP1A and MAP1B. *J.Biol.Chem.* **269:** 11492-11497.

Mann, S.S., and J.A.Hammarback. 1996. Gene localization and developmental expression of light chain 3: a common subunit of microtubule-associated protein 1A (MAP1A) and MAP1B. *J.Neurosci. (Rs.)* **43:** 535-544.

Margolis, L., and D.Job. 1994. Microtubule stabilization. In: Microtubules. Eds. Hyams, J.S., Clive, W.L., pp.221-228, Wiley-Liss, Inc., NY.

Matus, A. 1988. Microtubule-associated proteins: Their potential role in determining neuronal morphology. *Annu. Rev. Neurosci.* **11:**29-44.

Matus, A. 1994. MAP2. In: Microtubules. Eds. Hyams, J.S, Clive, W.L., pp. 155-166, Wiley-Liss, Inc., NY.

McKerracher, L., Vallee, R.B., and A.J.Aguayo.1989. Microtubule-associated protein 1A (MAP1A) is a ganglion cell marker in adult rat retina. *Visual Neurosci.***2:** 349-356.

Meixner, A., Haverkamo, S., Wassle, H., Fuhrer, S., Thalhammer, J., Kropf, N., Bitner, R., Lassmann, H., Wiche, G., and F. Propst. 2000. MAP1B is required for axon guidance, and is

involved in the development of the central, and peripheral nervous system. *J.Cell Biol.* **151:** 1168-1178.

Mitchison, T. and M. Kirscher. 1984. Dynamic instability of microtubule growth. *Nature* **312:** 237-313.

Müller, R., Kindler, S., and C.C.Garner. 1994. The MAP1 family. In Microtubules, eds. Hyams, J.S., Clive, W.L., pp. 141-154, Wiley-Liss, Inc., NY.

Nguyen, H.-L., Chari, S., Gruber, D., Lue, C.-M., Chapin, S.J., and J.C., Bulinski. 1997. Overexpression of full- or partial- length of MAP4 stabilizes microtubules and alters cell growth. *J.Cell Sci.* **110:** 281-294.

Noble, M., Lewis, S.A., and J.N.Cowan. 1989. The microtubule binding domain of microtubule-associated protein MAP1B contains a repeated sequence motif unrelated to that of MAP2 and tau. *J.Cell Biol.* **109:** 3367-3376.

Oblinger, M.M. and S.A.Kost. 1994. Coordinate regulation of tubulin and microtubule-associated protein genes during development of hamster brain. *Developmental Brain Res.* **77:**45-54.

Olson, K.R., McIntosh, J.R., and J.B. Olmsted. 1995. Analysis of MAP4 function in living cells using green fluorescent protein GFP) chimeras. *J.Cell Biol.* **130:** 639-650.

Pedrotti, B., Soffientini, A., and K. Islam. 1993. Sulphonate buffers affect the recovery of microtubule-associated proteins MAP1 and MAP2: evidence that MAP1A promotes microtubule assembly. *Cell Motil. Cytoskeleton* **25:** 234-242.

Pedrotti, B., and K. Islam. 1994. Purified native microtubule-associated protein MAP1A: kinetics of microtubules assembly and MAP1A/tubulin stoichiometry. *Biochemistry* **33:** 12463-12470.

Pedrotti, B., Colombo, R., and K. Islam. 1994. Microtubule-associated protein MAP1A is an actin-binding and crosslinking protein. *Cell Motil.Cytoskeleton* **29:** 110-116.

Pedrotti, B., and K. Islam. 1996. Dephosphorylated but not phosphorylated microtubule-associated protein MAP1B binds to microfilaments. *FEBS (Fed. Eur. Biochem. Soc.) Lett.* **388:** 131-133.

Pedrotti, B., Ulloa, L., Avila, J., and K.Islam. 1996a. Characterization of microtubule-associated proteins MAP1B: phosphorylation state, light chains, and binding to microtubules. *Biochemistry* **35:** 3016-3023.

Pedrotti, B., Francolini, M., Cotelli, F., and K.Islam. 1996b. Modification of microtubule shape *in vitro* by molecular weight microtubule-associated proteins MAP1A, MAP1B and MAP2. *FEBS (Fed. Eur.*

Biochem. Soc.) Lett. **384:**147-150

Riederer, B., and A.Matus. 1985. Differential expression of distinct microtubule-associated proteins during brain development. *Proc.Natl. Acad. Sci. USA.* **82:** 6006-6009.

Riederer, B.M. 1990. Some aspects of neuronal cytoskeleton in development. *Eur. J. Morphol.* **28:** 347-378.

Sambrook, J., Fritsch, E.F. and T.Maniatis. 1989. Molecular Cloning: a laboratory manual, Vol. I. Cold Spring Harbor Laboratory Press, Cold Spring Harbor.

Sato-Yoshitake, R., Shiomura, Y., Miyasaka, H., and N.Hirokawa. 1989. Microtubule-associated protein 1B: molecular structure, localization, and phosphorylation-dependent expression in developing neurons. *Neuron* **3:** 229-238.

Schoenfeld, T.A., McKerracher, L., Obar, R., and R.B. Vallee. 1989. MAP1A and MAP1B are structurally related microtubule-associated proteins with distinct developmental patterns in the CNS. *J.Neurosci.* **9:** 1712-1730.

Schoenfeld, T. A. and R. A. Obar. 1994. Diverse distribution and function of fibrous microtubule-associated proteins in the nervous system. *Int.Rev. Cytol.* **151:** 67-137.

Shiomura, Y., and N.Hirokawa. 1987. The molecular structure of

microtubule-associated protein 1A (MAP1A) *in vivo* and *in vitro*. An immunoelectron microscopy and quick-freeze, deep-etch study. *J. Neurosci.* **7:** 1461-1469.

Steffanini, M. DeMartino, C. and L.Zamboni. 1967. Fixation of ejaculated spermatozoa for electron microscopy. *Nature* **216:** 173-174.

Svitkina, T.M., Verkhovsky, A.B., and G.G.Borisy. 1996. Plectin sidearms mediate interaction of intermediate filaments with microtubules and other components of the cytoskeleton. *J.Cell Biol.* **135:** 991-1007.

Takei, Y., Kondo, S., Harada, A., Inomata, S., Nooda, T., and N. Hirokawa. 1997. Delayed development of nervous system in mice homozygous for disrupted microtubule-associated protein 1B (MAP1B) gene. *J.Cell Biol.*, 1615-1627.

Takemura, R., Okabe, S., Umeyama, T., Kanai, Y., Cowan, N.J., and N.Hirokawa. 1992. Increased microtubule stability and alpha tubulin acetylation in cells transfected with microtubule-associated proteins MAP1B, MAP2 and tau. *J.Cell Sci.* **103:** 953-964.

Thrower, D., Jordan, M.A., and L. Willson. 1991. Quantitation of cellular tubulin in microtubules and in tubulin pools by competitive ELISA. *J. Immunol. Meth.* **136:** 45-51.

Towbin, H., Staehlin, T., and J.Gordon. 1979. Electrophoretic transfer of

proteins from polyacrylamide gels to nitrocellulose sheets: procedure and some applications. *Proc. Natl. Acad. Sci. U.S.A.* **76:** 4350-4354.

Tögel, M., Wiche, G., and F.Propst. 1998. Novel features of the light chain of microtubule-associated protein MAP1B : Microtubule stabilization, self interaction, actin filament binding, and regulation of the heavy chain. *J. Cell Biol.* **143:** 697-707.

Ulloa, L., Avila, J., and J.Diaz-Nido. Microtubule-associated protein 1B (MAP1B): A key regulator in neuritogenesis. In Brain microtubule associated proteins. Modifications in Disease. eds. Avila, J. Brandt, R., and K.S. Kosik, pp.17-31. Harwood Academic Publishers, Canada.

Vaillant, A.R., and D.L. Brown. 1995. Accumulation of microtubule-associated protein 1A (MAP1A) in differentiating P19 embryonal carcinoma cells. *Biochem. Cell Biol.* **73:** 695-702.

Vaillant, A.R. 1997. Microtubule-assoicated protein 1a: analysis of its microtubule binding domain and its function in differentiating P19 neurons. *Ph.D. thesis,* Ottawa, Canada.

Vaillant, A.R., Müller, R., Langkopf, A., and D.L.Brown. 1998. Characterization of the microtubule-associated protein 1A and its effects on microtubule dynamics. *J.Biol. Chem.* **273:** 13973-13981.

Vale, R. D. 1990. Microtubule-based proteins. *Curr. Opin.Cell Biol.* **2:** 15-22.

Vallee, R.B., and S.E., Davis. 1983. Low molecular weight microtubule-associated proteins are light chains of microtubule-associated protein 1(MAP 1). *Proc. Nalt. Acad. Sci. USA.* **80:** 1342-1346.

Weisshaar, B., Doll, T., and A.Matus. 1992. Reorganization of the micro-tubular cytoskeleton by embryonic microtubule-associated protein 2 (MAP2c). *Development* **116:** 1151-1161.

Wiche, G., Oberkanins, C., and A.Himmler. 1991. Molecular structure and function of microtubule-associated proteins. *Int. Rev. Cytol.* **124:** 217-273.

Wooten, jG.F., Kopin, I.J., and J.Axelrod. 1975. Effects of colchicine and vinblastine on axonal transport and transmitter release in sympathetic nerves.*Ann. NYAcad. Sci.* **253:** 528-534.

Wordeman, L. and T.J.Mitchison. 1994. Dynamics of microtubule assembly *in vivo.* In Microtubules, eds. Hyams, J.S. and W.L. Clive. pp.287-301, Wiley-Liss, Inc., NY.

Xiang, H. and T.H. MacRae. 1995. Production and utilization of detyrosinated tubulin in developing *Artemia larvae*: Evidence for a tubulin-reactive carboxypeptidase. *Biochem. Cell Biol.* **71:** 673-685.

Zauner, W., Kratz, J., Staunton, J., Feick, P., and G. Wiche. 1992.

Identification of two distinct microtubule binding domains on recombinant rat MAP1B. *Eur. J. Cell Biol.* **57:** 66-74.